Geoscience Frontiers 7 (2016) 715–731

HOSTED BY

Contents lists available at ScienceDirect

China University of Geosciences (Beijing)

Geoscience Frontiers

journal homepage: www.elsevier.com/locate/gsf

Research paper

Early Permian arc-related volcanism and sedimentation at the western margin of Gondwana: Insight from the Choiyoi Group lower section

Leonardo Strazzere, Daniel A. Gregori*, Leonardo Benedini

CONICET and Cátedra de Geología Argentina, Departamento de Geología, Universidad Nacional del Sur, San Juan 670, 8000 Bahía Blanca, Argentina

ARTICLE INFO

Article history:
Received 4 January 2015
Received in revised form
7 August 2015
Accepted 31 August 2015
Available online 19 October 2015

Keywords:
Choiyoi group lower section
Conglomerado del Río Blanco
Cordillera Frontal
Argentina

ABSTRACT

Permian sedimentary and basic to intermediate volcanic rocks assigned to the Conglomerado del Río Blanco and Portezuelo del Cenizo Formation, lower part of the Choiyoi Group, crop out between the Cordon del Plata, Cordillera Frontal and Precordillera of Mendoza Province, Argentina. The sedimentary rocks are represented by six lithofacies grouped in three facies associations. They were deposited by mantled and gravitational flows modified by high-energy fluvial currents that evolved to low-energy fluvial and lacustrine environments. They constitute the Conglomerado del Río Blanco, which cover unconformably marine Carboniferous sequences. Five volcanic and volcaniclastic facies make up the beginning of volcanic activity. The first volcanic event in the Portezuelo del Cenizo is basaltic to andesitic lava-flows emplaced in the flanks of volcanoes. Lava collapse produced thick block and ash flows. Interbedding in the intermediate volcanic rocks, there are dacites of different geochemical signature, which indicate that the development of acidic volcanism was coetaneous with the first volcanic activity. The geochemistry of these rocks induces to consider that the Choiyoi Group Lower section belongs to a magmatic arc on continental crust. The age of this section is assigned to the lower Permian (277 ± 3.0 Ma, Kungurian age).

© 2015, China University of Geosciences (Beijing) and Peking University. Production and hosting by Elsevier B.V. This is an open access article under the CC BY-NC-ND license (http://creativecommons.org/licenses/by-nc-nd/4.0/).

1. Introduction

Basic to felsic igneous rocks were emplaced and extruded along the western margin of the Gondwana supercontinent, during late Paleozoic and early Triassic times. The rocks form a belt, more than 2500 km long of plutonic, volcanic, and subvolcanic rocks.

This igneous rocks crop out in the Eastern Cordillera of Peru and the Andes of Chile, mainly in the Domeyko and Elqui-Limarí Cordilleras (Hervé et al., 2014; Maksaev et al., 2014). In Argentina, main outcrops are in the Cordillera Frontal, Cordillera Principal, and the Precordillera (Fig. 1).

The ages obtained by the above cited authors and Parada Velazquez (2013) indicate three different events: upper Carboniferous (323–307 Ma), lower Permian (287–264 Ma) and middle Triassic (232–221 Ma). The older event is a subduction-related magmatism, whereas the later correspond to a within-plate, related to extensional conditions.

All of these groups are represented in Argentina, but the 287–264 Ma magmatic event crops out in a wider area (>500,000 km^2), from the La Rioja Province to the Neuquén Province. Fig. 1 displays the area between San Juan and the central part of Mendoza Province.

This intense igneous activity is known as the Choiyoi magmatic province (Kay et al., 1989).

Groeber (1946, 1951), Polanski (1958, 1964), Caminos (1965), Stipanicic et al. (1968) and Rolleri and Criado Roque (1970) reported the first regional information about this magmatism. They proposed a stratigraphy pile composed of sedimentary sequence at the base followed upwards by basaltic-andesitic volcanic facies and then, transitionally, dacite and rhyolite facies, assigned them to the Choiyoi Group.

New contributions by Kay et al. (1989), Mpodozis and Kay (1992), Llambias et al. (1993), Poma and Ramos (1994), Llambías et al. (2003), Strazzere and Gregori (2005), Strazzere et al. (2006), Kleiman and Japas (2009) among others, indicate that the basaltic-andesitic facies is subduction-related.

* Corresponding author. Tel.: +54 291 4595101x3031.
E-mail addresses: lstrazze@uns.edu.ar (L. Strazzere), usgregor@criba.edu.ar (D.A. Gregori), lbenedini@criba.edu.ar (L. Benedini).
Peer-review under responsibility of China University of Geosciences (Beijing).

http://dx.doi.org/10.1016/j.gsf.2015.08.009
1674-9871/© 2015, China University of Geosciences (Beijing) and Peking University. Production and hosting by Elsevier B.V. This is an open access article under the CC BY-NC-ND license (http://creativecommons.org/licenses/by-nc-nd/4.0/).

The upper section evolves to shoshonitic and high-K calc-alkaline series, indicative of extensional regime (Strazzere et al., 2006).

The volcanism of the Choiyoi Group originates from megafaults resulting from the notable anisotropy of the upper crust that controls the tectonic patterns (Giambiagi and Martinez, 2008). The emplacement and distribution of the first volcanic event seems to be related to these tectonic patterns, developed in part due to an important deformational event known as San Rafael diastrophic phase (Llambias and Sato, 1990, 1995; Llambias et al., 1993; Heredia et al., 2002). This volcanic event marks the beginning of the Permian volcanism that according to Llambías and Sato (1990, 1995) and Llambias et al. (1993) lasted more than 40 Ma.

Since the best outcrops of the Choiyoi Group are located on the eastern slope of the Cordon del Plata (Cordillera Frontal) and in the western slope of the Precordillera of Mendoza, this sector was chosen in order to carry out stratigraphical, geochemical and geochronological studies (Figs. 1 and 2).

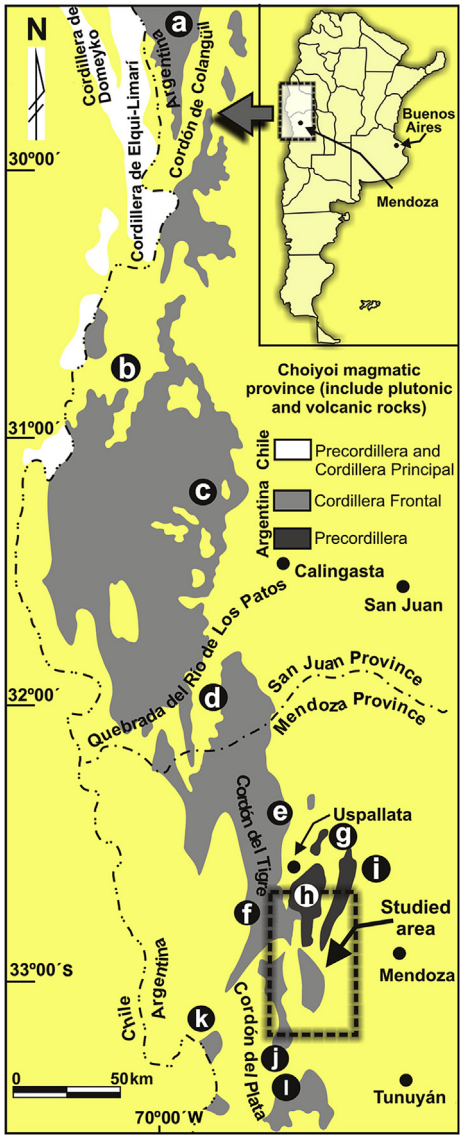

Figure 1. Choiyoi magmatic province cropping out in Chile and Argentina. Dotted line shows the location of the study area. The Cordillera Frontal and Precordillera of Mendoza and San Juan provinces. (a) Cordillera de Colangüil, Sato and Llambías (1993); (b) Cordillera Frontal between 30°00′ and 31°30′S, Heredia et al. (2002); (c) Cordillera Frontal, western of Calingasta, Caballé (1990); (d) Valle del Río de Los Patos, Mirré (1966); (e) Cordillera del Tigre, Coira and Koukharsky (1976); (f) Estancia Tambillos, Cortés (1985); (g) Cerro Cantera, Pöthe de Baldis (1975); (h) Quebrada de Santa Elena and Telégrafo, Strazzere et al. (2006); (i) Sierra de Mal País, Harrington (1941); (j) North-eastern side of Cordón del Portillo, González Díaz (1957); (k) Alto Río Tupungato, Fernández (1955); (l) Cordón del Portillo, Poma and Ramos (1994).

In order to understand the evolution of the Choiyoi Group and the mechanisms of the volcanism and extrusion, detailed geological mapping and 11 stratigraphic profiles were carried out.

The objective of this study is to provide new geological descriptions, geochemical and geochronological data that allow to establish the evolution of the Choiyoi Group. Based on this data, we explain the geotectonic environments in which the volcanism was developed.

The aim of this paper is to contribute to the understanding of the tectonic setting of the volcanic and sedimentary rocks of the Choiyoi Group based on geological mapping, sampling, carried out on these volcanic sequence cropping out in the eastern area of the Cordón del Plata and Precordillera of Mendoza.

In view of that, comparisons with equivalent rocks of similar age from the Cordillera Frontal of Argentina and Precordillera of Mendoza are made to model the evolution of this sector of the Gondwana continental margin.

2. Geology of the study area

The studied area is located between 69°08′W–33°00′S and 69°22′W–32°44′S (Figs. 1 and 2). The older rocks are located in the northern and central part of Fig. 2. Those located in the northern part corresponds to tectonically-emplaced slices of low-degree metamorphic rocks with interbedded basalts and ultramafic bodies assigned to the Bonilla Formation (Borrello, 1969; Varela, 1973; Folguera et al., 2004; Gregori et al., 2013). This unit can be correlated with the Guarguaraz Complex (López and Gregori, 2004; Lopez de Azarevich et al., 2009; Willner et al., 2011), cropping out in the Cordón del Plata.

In the central part the Cambrian Cerro Pelado Formation, it is composed of marine sedimentary rocks deposited in an internal calcareous platform described by Heredia (1990, 1996). The southeastern, crops out a sedimentary sequence of interbedded green shales with small limestones bodies (Fig. 2), originally assigned to the Ordovician and named Villavicencio Formation (Harrington, 1941; Kury, 1993).

However, detail studies carried out by Cuerda (1988) and Rubinstein and Steemans (2007) indicate a late Pragian to early Emsian age (~407 Ma, lower Devonian), reassigned to the Canota Formation by these authors.

The upper Carboniferous–lower Permian age is represented by outcrops (Fig. 2) of the Loma de los Morteritos and El Plata formations (Polanski, 1958). They are composed by interbedding of fine-grained arkoses and siltstones more than 750 m thick (Figs. 2 and 3b). Ripple marks and sigma structures due to migration of sandy bars are common in the sequence. Siltstones show lateral discontinuity, disappearing in short distance. Conglomerates are scarce.

Deformation is complex and exhibit kink bands and metric to kilometric chevron folding. Determinations of palynomorphs indicate upper Carboniferous–lower Permian age (Azcuy, 1993; Sabattini, 1993; Azcuy et al., 1999). The age of sedimentation of the marine basin extended up to Sakmarian-Kungurian times (295–272 Ma) according to Pagani and Sabattini (2002). According to Taboada (2001) sedimentation continues until Asseliane-Sakmarian (~299–284 Ma).

In the Cerro Médanos a roof-pendant of Carboniferous rocks is located over the plutonic rocks, whereas in the Quebrada Angostura the Bonilla Formation and the Carbonifeorus marine rocks is overthrusted by the granitic rocks (Fig. 2).

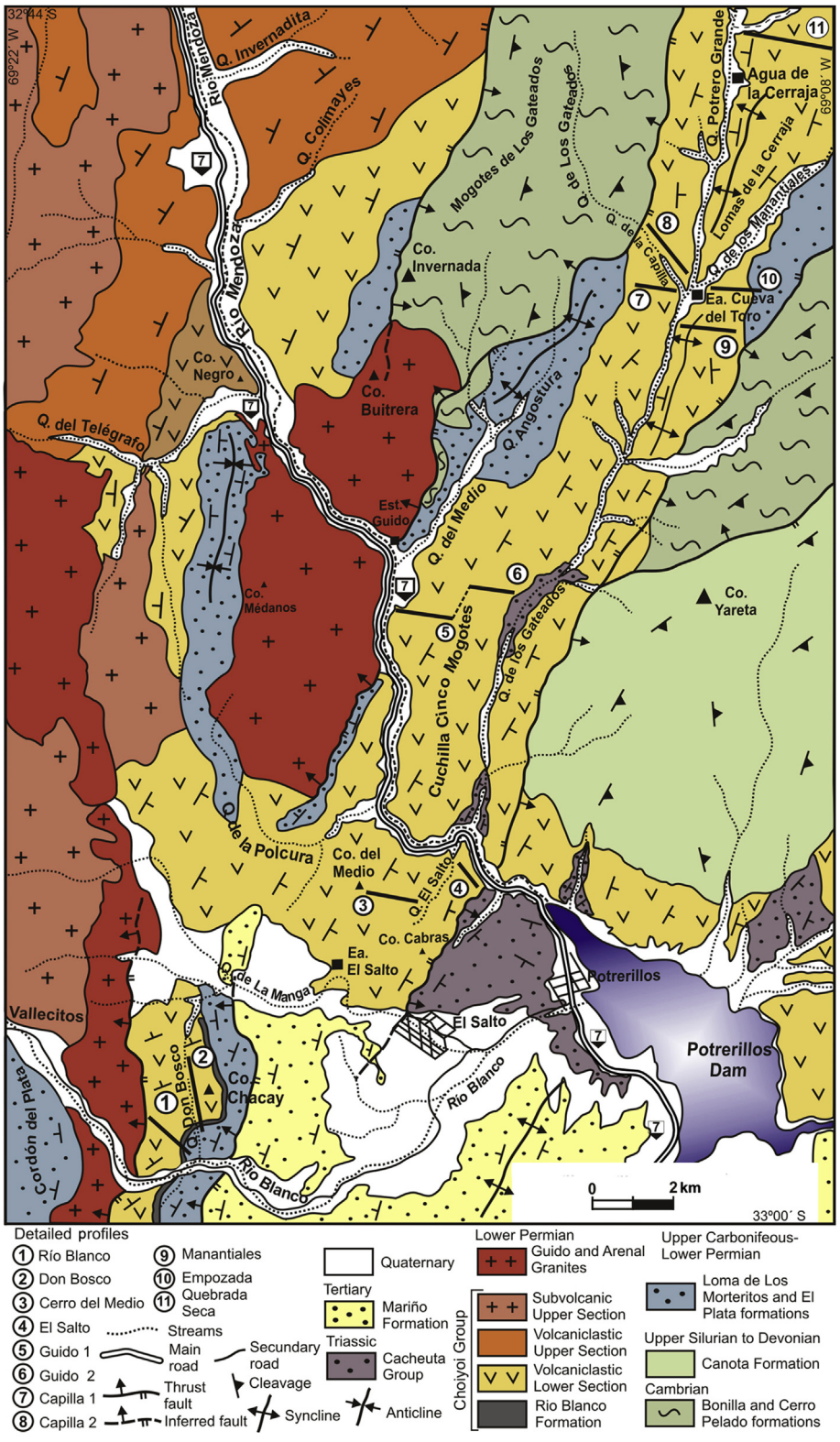

Figure 2. Geologic map of the study area according with own field recognizement. Location of profiles is displayed.

The Conglomerado del Río Blanco, that forms the lower part of the Choiyoi Group, crop out in the eastern side of Cerro Chacay and in the Quebrada de Don Bosco (Fig. 2). In this area the non-conformity surface between this unit and the Loma de los Morteritos Formation is evident (Figs. 2 and 3a, b). According to field relationships the age of Choiyoi Group must be earlier than upper Carboniferous–lower Permian.

Tuffs, lava-flows and andesitic breccias are interbedding in the conglomerates and sandstones of this unit (Fig. 3, profile). The structure is relatively simple and consists of strata dipping to the

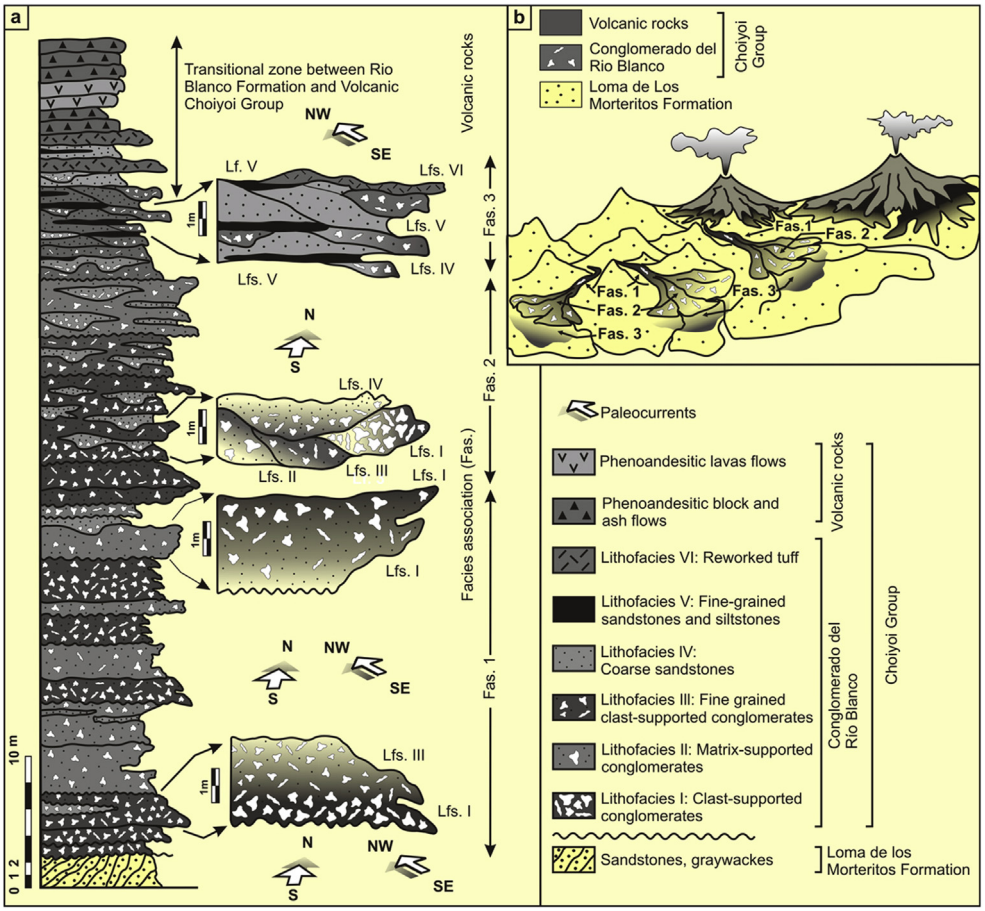

Figure 3. (a) Profile of the Conglomerado del Río Blanco located in the left side of the Río Blanco. (b) Schematic representation for the possible relationships between the facies associations. The sediments are accommodated in thick laterally discontinuous deposit.

NW. The conglomerates and sandstones continue transitionally to the volcanic sequences of the Choiyoi Group lower section (Figs. 3a and 4a, c, d, and e). It is composed of andesitic block and ash flows, phenoandesitic lava-flows, andesitic autobreccias and pyroclastic flows of dacitic composition.

They were assigned to the basic-intermediate section by Caminos (1965), Strazzere and Gregori (2005) and Strazzere et al. (2006). The Choiyoi Group upper section (Fig. 2) is represented in its base by scattered and thin ignimbritic levels that upwards are composed predominantly by massive ignimbritic levels and rhyolitic domes.

The granitic, aplitic and rhyolitic dykes of the Cerro Arenal Stock (Fig. 2), intrude all units (Caminos, 1965; Orme et al., 1996).

The younger limit of the Choiyoi Group was recognized few kilometers north of Potrerillos, where continental sedimentary rocks of the Triassic Cacheuta Group unconformably cover lava-flows of the Choiyoi Group.

The Triassic Cacheuta Group represents rift deposits that include granitic cobles derived from the Cerro Arenal Stock and Guido Granite. U/Pb dating of the Rio Blanco basin, equivalent to the Cacheuta Group indicates ages of 246 and 230 Ma (Barredo et al., 2012).

Tertiary and Quaternary rocks are represented by alluvial deposits of the Oligocene–Miocene Mariño Formation overthrusted on the Loma de los Morteritos Formation (Fig. 2).

3. Stratigraphy of the Choiyoi Group lower section

Historically, the Choiyoi Group was divided into three sections: lower, mainly basaltic; middle, andesitic; and upper of dacitic-rhyolitic composition (Polanski, 1958, 1964; Caminos, 1965; Rolleri and Criado Roque, 1970). This division excludes the conglomerates and sandstones located unconformably over the upper Carboniferous–lower Permian marine sequences. This unit was named Conglomerado del Río Blanco by Caminos (1965), whereas the basaltic-andesitic section was named Portezuelo del Cenizo Formation by Coira and Koukharsky (1976).

In this paper, we include the Conglomerado del Rio Blanco in the Choiyoi Group because this sedimentary unit is transitional to the volcanic rocks. Therefore, the Choiyoi Group lower section is composed by sedimentary facies, the Conglomerado del Río Blanco and volcanic facies, the Portezuelo del Cenizo Formation. Llambias et al. (1993) were the first authors that include the Conglomerado del Rio Blanco in the Choiyoi Group.

3.1. Conglomerado del Río Blanco

Two detailed profiles (40–60 m thick) were carried out in order to determine facies association and environments (Figs. 2–4). The profiles are located in the western side of Cerro Chacay (Cerro Chacay profile, Fig. 2) and in the western side of Quebrada de Don Bosco (Don Bosco profile, Fig. 2).

The outcrops are located along the eastern slope of the Cordon del Plata and can be followed for more than 4 km. The average thickness is between 60 and 70 m although local depocenter can reach 150 m thick.

During the analysis of the detailed profiles of the Conglomerado del Río Blanco six lithofacies (Lfs) were recognized (Table 1).

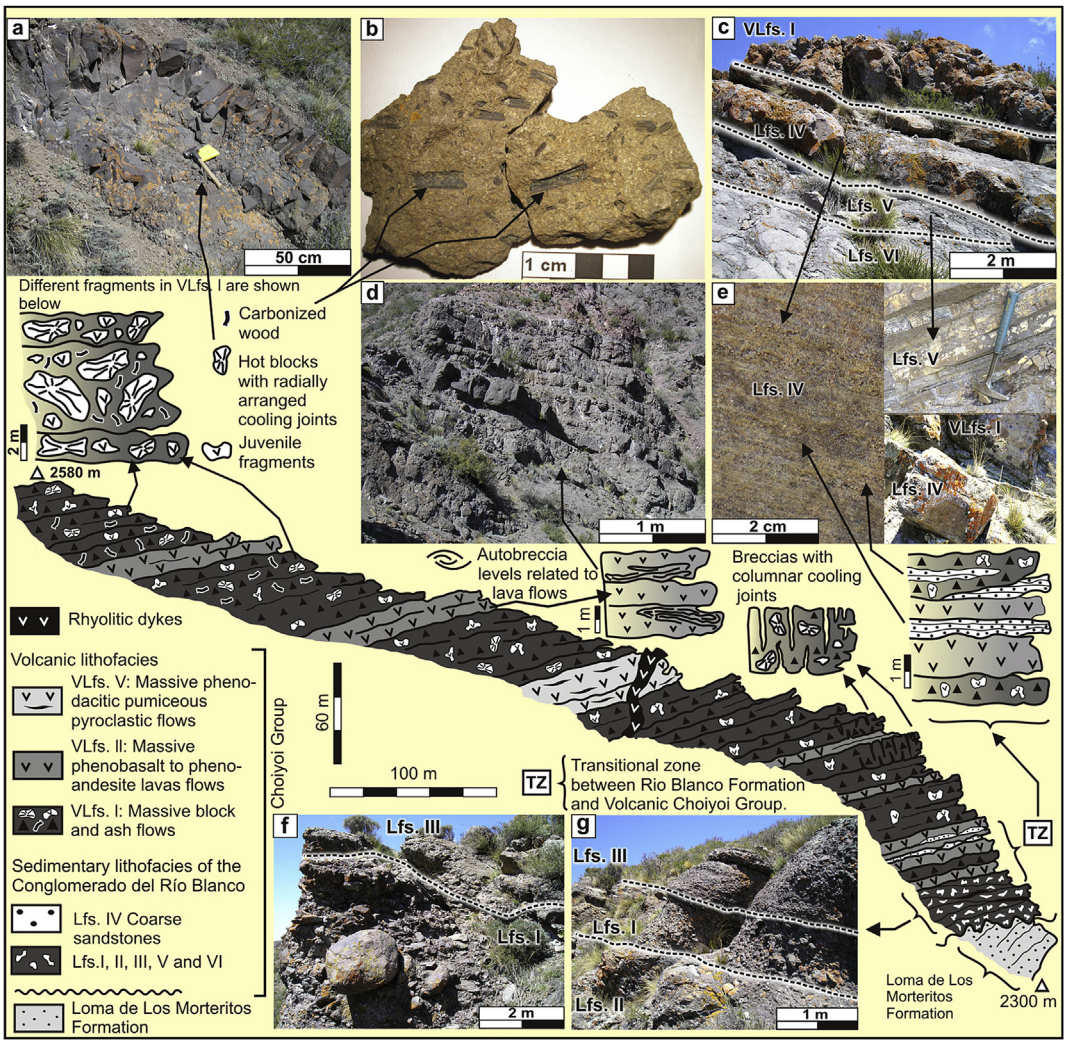

Figure 4. Don Bosco profile showing the contact between Loma de Los Morteritos Formation, the Conglomerado del Río Blanco and its transition to the Choiyoi Group lower section. (a) Hot blocks with radially arranged cooling joints included in a block and ash flow. (b) Carbonized wood found in the block and ash flows. (c) Interbedding of siltstones, low-energy channelized flows and reworked tuffaceous material. Upwards volcanic breccias and scarce lavas belonging to the Choiyoi Group Lower section cover the sedimentary units. (d) Succession of thin basaltic to andesitic lava flows. (e) Interbedding of siltstones, reworked tuffaceous material and coarse sandstones. (f, g) Interbedding of clast-supported, matrix-supported and fined-grained conglomerates. Clasts up to 1 m diameter can be found.

Lithofacies I is composed of clast-supported conglomerates (Figs. 3a and 4f, g), whereas lithofacies II is represented by matrix-supported conglomerates (Figs. 3a and 4g). Fine-grained clast-supported conglomerates (Figs. 3a and 4f, g) and coarse sandstones correspond to lithofacies III and lithofacies IV (Figs. 3a and 4c, e) respectively. Upwards appears fine-grained sandstones and siltstones (Figs. 3a and 4c, e) of lithofacies V and reworked tuff (Figs. 3a and 4c) of lithofacies VI.

3.1.1. Facies association

Three facies associations were recognized in the Conglomerado del Rio Blanco. Lithofacies I to III represent the first facies association and indicate decreasing energy in fining-upwards mantled flows (Fig. 3b).

The assemblage of high-density alluvial flows defined by lithofacies II represents the second facies association. They correspond to massive bodies (50 cm–1 m thick) of rough coarsening-up sequences (Figs. 3a and 4g). Both types of alluvial fans suggest scarce participation of aqueous phase and sedimentation in a high-gradient topographic scenario located near the source of sediments. Due to the absence of fluvial reworking at the top of the banks, we consider that the time in between each sedimentary event was short.

The last section of the profile shows interbedding of siltstones and coarse sandstones up to 1 m thick that represents facies association III, typical of low-energy channelized flows (lithofacies IV and V, Figs. 3a and 4c, e).

Reworked tuffs (lithofacies VI, Figs. 3a and 4c) were deposited in small water ponds where decantation of fine material and preservation of volcanic ash occur. Presence of pyrite crystal in siltstones and tuffs indicates reduced conditions.

Interbedding conglomerates (lithofacies I and II) indicate alluvial fans due to tectonic reactivation on a local scale. The presence of volcanic breccias and scarce lava-flows of the Portezuelo del Cenizo Formation interbedded in the Conglomerado del Río Blanco, suggest that both units are transitional and partly coeval (Figs. 3a, b and 4c, e).

The thickness variations, the lateral changes in channelized and mantled flows and as well as the analyses of facies association suggest a significant irregular topography of the basin, with source areas located south and southeast and paleoflows directed north and northwest (Fig. 3a, b).

Table 1
Principal characteristics of lithofacies of the Conglomerado del Río Blanco.

Lithofacies	Name	Shape	Relation clast/groundmass	Clast dimensions and compositions	Matrix compositions	Paleocurrents
I	Clast-supported conglomerates	5–20 m, clastic wedges	85%/15%	10–30 cm up to 1 m; sandstones, quartz and pelites	Coarse sandstone of arkoses, pelites and white quartz	Imbricate clasts from SW, cross stratification to N–NW
II	Matrix-supported conglomerates	1–2 m, tabular bodies	60%/40%	5–20 cm up to 50 cm; sandstones, quartz and pelites	Coarse-grained sandstone; fragment of schists, greywackes and quartz	Imbricate clasts from SW, cross stratification from N–NW.
III	Fine-grained clast-supported conglomerates	2–5 cm, tabular beds	75%/25%	2–5 cm; sandstones, siltstones and volcanic porphyritic rocks	–	–
IV	Coarse sandstones	60–80 cm, tabular beds	–	1–2 mm; milky quartz and siltstones	–	Cross stratification from N–NW
V	Fine-grained sandstones and siltstones	20–40 cm, lenticular shape	–	–	–	–
VI	Reworked tuffs	25–35 cm massive beds	–	1–3 mm; volcanic porphyritic rocks and euhedral pirites	–	–

3.2. Portezuelo del Cenizo Formation

The volcanic and volcaniclastic rocks of the Portezuelo del Cenizo Formation conform a continuous NNE–SSW belt (Fig. 2) located conformably on the Conglomerado del Río Blanco (Fig. 3a) and unconformably on the Loma de los Morteritos Formation in the western side of Cerro Chacay. In this area, the Conglomerado del Río Blanco rest on a surface dipping 30° to the northwest on the folded Loma de Los Morteritos Formation (Fig. 2).

Along the Cuchilla Cinco Mogotes and until Estancia Cueva del Toro, the Portezuelo del Cenizo Formation covers unconformably the marine sedimentary rocks and dips 20°–35° SE.

Along the NNE–SSW belt of the Portezuelo del Cenizo Formation, eleven detailed profiles were measured (Fig. 2), allowing recognition of five volcanic lithofacies (VLfs.). From those, five are depicted and was used to interpret eruptive styles and the development of the volcanism (Table 2). In small depocenters interbedded in the volcanic rocks, four sedimentary lithofacies were also recognized (Table 3).

Although some sedimentary facies look similar to those observed in the Conglomerado del Río Blanco, the clasts and matrix composition are different, being necessary a different nomenclature (SLfs.).

The volcanic lithofacies (VLfs.) can be divided as follows: the VLfs. I is basic breccias (Figs. 4a, b and 5b); the VLfs. II is represented by massive phenobasalt to phenoandesite lava flows (Figs. 4d and 6a, b); and VLfs. III is massive phenoandesite to phenodacite lava flows (Figs. 6c and 7b, c, d); VLfs. IV is represented by agglomerates and is displayed in Fig. 5a; whereas VLfs. V is massive phenodacitic pumiceous pyroclastic flows (Figs. 6d, e and 7a, d).

3.2.1. Eruptive styles

Three different eruptive styles were recognized during facies analysis. Two are genetically related, mostly represented in the Cordón del Plata and the Cuchilla de los Cinco Mogotes, whereas the other belongs to a volcanism of different composition located near Quebrada de Los Manantiales and Cueva del Toro. The first style corresponds to the eruption of phenobasaltic to phenoandesitic lava-flows (VLfs. II and III, Figs. 4–7). The emplacement of this type of flow requires low content of dissolved gas in the magma or releases from a magmatic chamber prior to eruption.

There is a transition between intersertal-intergranular olivine basalts and trachytic texture andesites and dacites with up to 30% phenocrysts (VLfs. III, Figs. 6 and 7). The last are more common in the central-north part of the studied area. Autobreccia levels are closely related to this type of eruption and some agglomerate levels are linked to the lava-flows (VLfs. IV, Fig. 5a).

The second volcanic style consists of block and ash flows (Cas and Wright, 1993), lava debris flows or hot avalanches deposits of Francis et al. (1974) (VLfs. I, Figs. 4 and 5).

They are represented by pyroclastic flows of small volume and scarce lateral development, up to 200 m long, generated by lava-dome collapse and lava collapse (Cas and Wright, 1993). Due to the absence of domes in this area, the collapse of lava-flows, located in the flanks of the volcanoes is assigned to this type of deposit. The volcanic fragments were generated without an important participation of volatiles. The existence of radial-curved joints and breadcrust textures in several profiles indicates that the volcanic flows are of high temperature. Some agglomerate levels are closely related to the block and ash flow deposits (VLfs. IV, Fig. 5a).

The third volcanic style is of phenodacitic to phenorhyolitic composition and the elevated proportion of vesiculated material implicates that a viscous magma with high quantity of volatiles was release during eruption.

The disposition covering an irregular topography, as well as, the homogeneity of this deposit is proper of a volatile rich, high temperature, pyroclastic flow, with high-welded glass. This conclusion is supported by the high content of fine vesiculated material deposited at elevated temperature allowing glass compactation and fiammes formation, typical of this volcanic event (VLfs. V, Figs. 6 and 7).

At the base of the ignimbrites levels were recognized breccias that are interpreted as co-ignimbrite lag breccias and occurred during the moving of pumiceous flows with a progressive segregation of lithic fragments (VLfs. V, Figs. 6 and 7).

It was recognized interbedding of pumiceous pyroclastic flows and massive phenobasaltic, phenoandesitic and phenodacitic lava, indicating that both types of volcanism were active during the same time.

On the other hand, the presence of volcanic fragments corresponding to VLfs. II and III (Figs. 6 and 7) suggests that the collapse of a column generated during an explosive eruption took place after the main lava-flow event.

Dacitic to rhyolitic pyroclastic volcanism was also described by Cortés et al. (1997), Strazzere and Gregori (2005) and Strazzere et al. (2006) in the Quebrada de Santa Elena and Quebrada del Telégrafo, located in the left side of the Mendoza river, 10 km away from the studied area.

Table 2
Principal characteristics of lithofacies of the Choiyoi Group lower section.

Volcanic lithofacies	Name	Shape and thickness	Fragments			Texture
			Type	Characteristic	Dimension	
I	Basic breccias	Planar base, 2–4 m thick	Non-vesiculate juvenile fragment of phenoandesites minor phenodacites; upwards, carbonized wood, accidental-accessory fragment are common	Rounded-shaped fragments with the same compositions of the groundmass; arrangements of curved radial joints; Breadcrust surface	2 cm–2 m	Most fragments have the same composition that de groundmass; trachytic texture with plagioclase, amphibole and pyroxene phenocrysts
II	Massive phenobasalt to phenoandesite lava flows	1 m thick with concentric exfoliations	Non-vesiculate juvenile fragments of phenoandesites located transitionally on bottom and top of the phenoandesitic lava flows	Fragment are due to fragmentation of frontal lava surface as cooling proceeds, and breaking of the lava flow bottom with consequent incorporation of fragments to the flow	0.4–1 m	Porphyry intersertal and glomerophyric texture with plagioclase, amphibole, pyroxene, and olivine phenocrysts in a glassy groundmass; amphibole and pyroxene are replaced by calcite, deep blue chlorite and epidote
III	Massive phenoandesite to phenodacite lava flows	1–2 m thick	Poor non-vesiculate juvenile fragments of phenoandesites	Lava fragments due to the cooling of the front surface and its continuous addition into the flow	2 cm–0.4 m	Porphyry to trachytic texture with plagioclase, amphibole, pyroxene phenocrysts and a glassy groundmass; amphibole and pyroxene are replaced
IV	Agglomerates	2–5 m thick	Poor non-vesiculate juvenile fragments of phenobasalt and andesites; bombs and ash	Rounded-shaped fragments with the same compositions of the groundmass; breadcrust surface	2–10 cm.	Fragment with trachytic texture of plagioclase; amphibole and pyroxene phenocrysts; altered olivine
V	Massive pumiceous phenodacitic pyroclastic flows	4–15 m thick	Vesiculate, pumiceous and vitroclastic fragments; phenoandesite to phenodacite fragments	Pumiceous and vitroclastic fragment are deformed forming eutaxitic textures	1–2 cm to 20 cm	Eutaxitic texture; euhedral phenocrysts of plagioclases and quartz are wrapped by deformed vitroclasts in a hialopilitic groundmass; zeolites and plagioclase were recrystallized in fiammes

3.2.2. *Epiclastic sequences related to the Portezuelo del Cenizo Formation*

The processes of erosion, transportation and redeposition of pyroclastic or effusive fragment were dominant during inter-eruption periods. The source of this material comes from the steep slope of volcanoes, topographic highs and volcanic piles.

Four sedimentary lithofacies (SLfs) were described and two facies associations were identified (Table 3). Lithofacies I (SLfs. I) is matrix-supported conglomerates; lithofacies II (SLfs. II) corresponds to coarse lithic sandstones (Fig. 5c), while fine-grained sandstones and siltstones (Fig. 5c) are lithofacies III (SLfs. III), and lithofacies IV (SLfs. IV) is dark crystalline limestone (Fig. 5d).

These accumulations of sediment are produced by gravitational collapse, mass-flows and running water from rivers and rain. This kind of depocenter is locally restricted and exclusively formed in a volcanic landscape, consequently clasts from oldest units are almost absent in the conglomerates.

3.2.3. *Sedimentary facies association*

In the Cuchilla Cinco Mogotes and Quebrada de los Manantiales profiles were recognized two facies associations.

Facies association I comprises lithofacies I, that represent alluvial fans formed by high-density gravitational flows. They are uniform and compact, with rude or absent stratification and may

Table 3
Principal characteristics of the sedimentary lithofacies of the Choiyoi Group lower section.

Sedimentary lithofacies	Name	Shape	Relationship clast/groundmass	Clasts dimension and compositions	Groundmass compositions	Flows directions
I	Coarse matrix-supported conglomerates	1–2 m tabular bodies	60%/40%	5–30 cm volcanic porphyritic rocks, fenodacites and fenoandecites	Coarse sandstone with angular-shaped	Flows from both, W and E directions; volcaniclastic sources
II	Coarse lithic sandstones	20–40 cm tabular beds with cross and parallel stratification	–	2–3 cm volcanic fragments, white quartz and minor sandstones	–	Cross stratification from SW
III	Fine-grained sandstones and siltstones	20–40 cm lenticular shape	–	2–5 cm; sandstones, siltstones and volcanic porphyritic rocks	Dark fine-grained sandstones	Cross stratification from SW–SE
IV	Dark crystalline limestones	40–60 cm lenticular shape with fine lamination and refolding textures	–	–	Green and black mud and gypsum levels	Cross stratification from N–NW

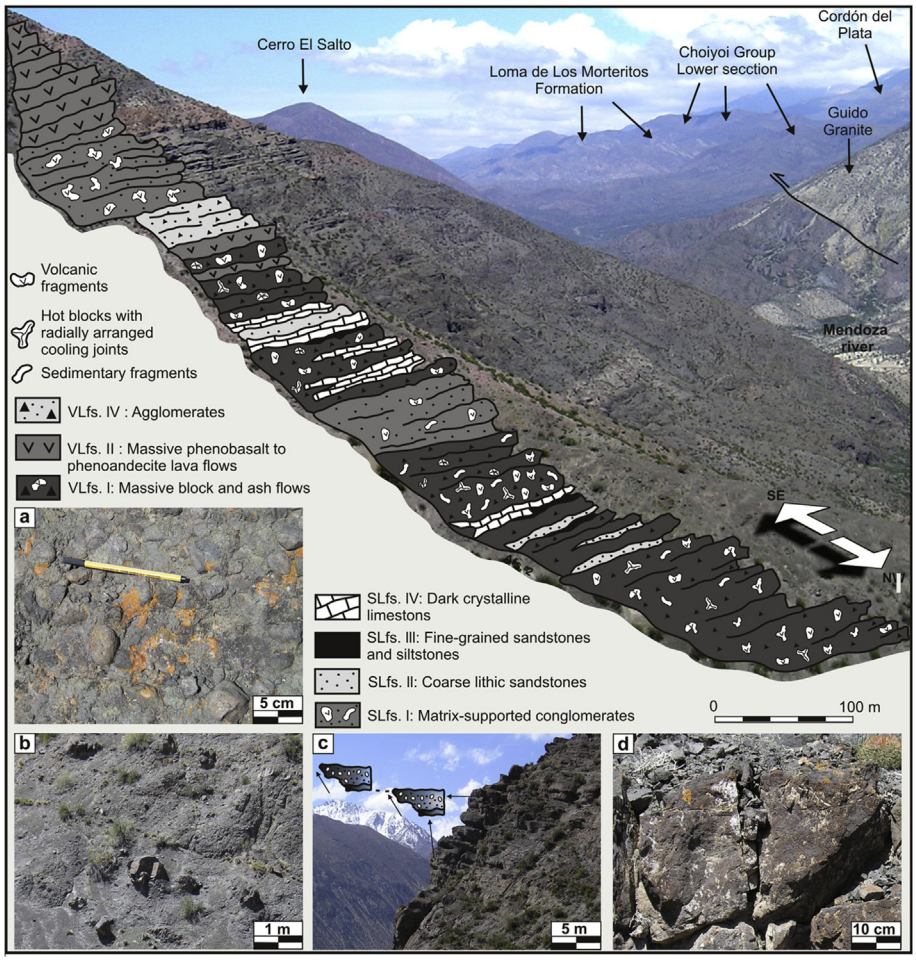

Figure 5. Guido profile and an overview of the east side of the Cordon del Plata showing the main outcrops of the Choiyoi group lower section. (a) Agglomerate levels; (b) hot blocks included in block and ash flow levels; (c) interbedding of fined-grained conglomerates with coarse siltstone bars belonging to epiclastic deposits; (d) dark crystalline limestone representing evaporitic lake facies.

present clast segregation in coarsening-upward sequences (Fig. 5c). This type of accumulation suggests considerable gradient and steep topographic, as well as, proximity to the areas of erosion with minimal participation of water flows. Periods between each depositional event seem to be long enough to allow the development of high-energy fluvial deposits that modify the fans roofs.

In some cases, amalgamated levels show lateral wedging, typical of alluvial fans.

Facies association II, that corresponds to the lithofacies II and III, shows fining-upward, channelized sequences, typical of low-energy flows. Profiles of erosion are characteristics and display erosive bases.

Clasts included in the channels correspond to altered dark basalts and andesites, while reworked volcanic material is common along the sequence. Sedimentary structures are poorly developed and correspond to parallel and cross-stratification.

These channelized low-energy flows, end in playa-lake environments or small depressions where mud and limestone of lithofacies III and IV were accumulated (Fig. 5d). The abundance of boulders identified as andesites and basalts of the Portezuelo del Cenizo Formation, together with subordinate Carboniferous sandstones and pelites suggests the existence of a paleorelieve developed on the volcanic and sedimentary sequences.

4. Geochemical composition of Portezuelo del Cenizo Formation

Geochemical analyses were carried on 18 representative samples for major, trace elements, and REE. Three samples represent basic breccias (block and ash flows), 7 samples are from massive phenoandesite flows, 3 from massive phenodacite lava-flows and 5 come from pumiceous phenodacitic pyroclastic flows. The analyses were performed using INAA and ICP-MS at ACTLABS (Canada). Major, trace and rare earth element data for the volcanic rocks are shown in Table 4.

4.1. Major elements

Due to the elevated values of LOI, the chemical classification based on major elements must be taken carefully. SiO_2 content varies between 52.31 and 70.30 wt.%, whereas K_2O and Na_2O are between 1.94–5.09 wt.% and 3.17–7.11 wt.% respectively. FeO^T oscillates between 2.29 and 8.01 wt.% and MgO is between 0.04 and 3.33 wt.% (Table 4). The rocks are andesites, dacites and rhyolites.

Harker diagrams (not shown) for the major elements display decreasing trends for Al_2O_3, P_2O_5, TiO_2, FeO, Fe_2O_3, CaO and MgO content with increasing SiO_2. K_2O and Na_2O have a positive trend with increasing SiO_2.

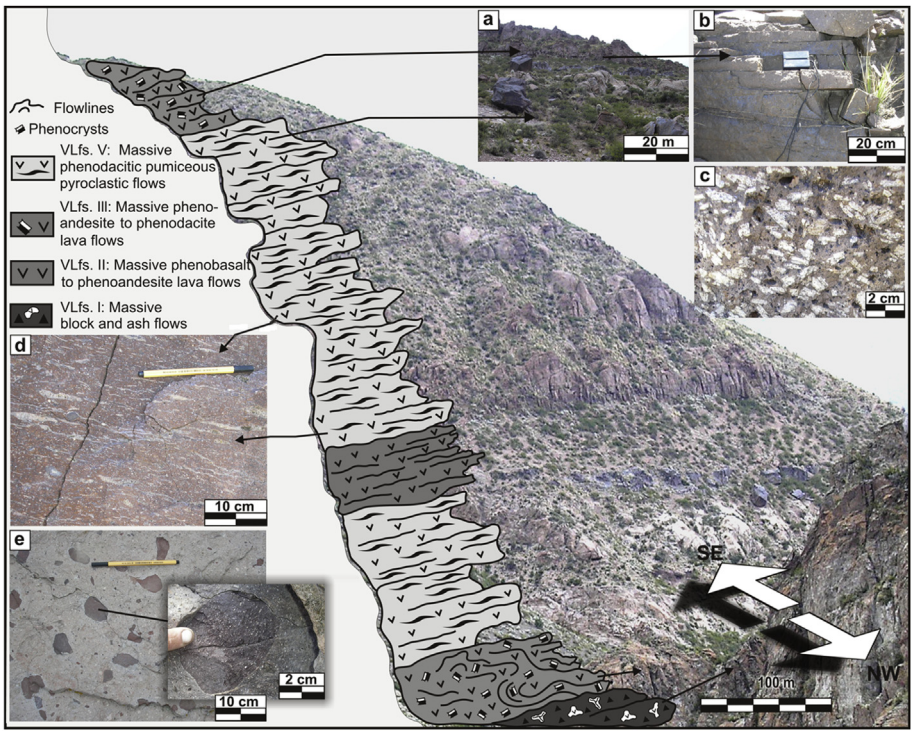

Figure 6. Quebrada de la Capilla profile. (a) Interbedding of crystals-rich andesite lava flows with massive dacitic pumiceous pyroclastic flows; (b) typical outcrops of crystals-rich andesite lava flows; (c) detailed view of the crystals-rich andesite lava flows; (d) Fiammes formation typical of the dacitic pumiceous pyroclastic flows; (e) crystals-rich andesite fragments included into the pumiceous pyroclastic flows.

Three distinctive groups of volcanic rocks can be observed in the TAS diagram of Le Maitre et al. (1989). The first group (VLfs. I and II) corresponds to basalts, trachyandesites, and andesites. The second group (VLfs. III) corresponds to trachytes and trachydacite and the last (VLfs. V) falls in both, trachydacite and rhyolite fields (Fig. 8a).

All the samples are potassium-rich in the Pecerrillo and Taylor's (1976) diagram (Fig. 8b) and most of the samples belong to the high-K series, from basandesites to rhyolites along a calc-alkaline trend. The same result was obtained in the AFM diagram of Irvine and Baragar (1971), where the samples displayed a calc-alkaline trend (Fig. 8c).

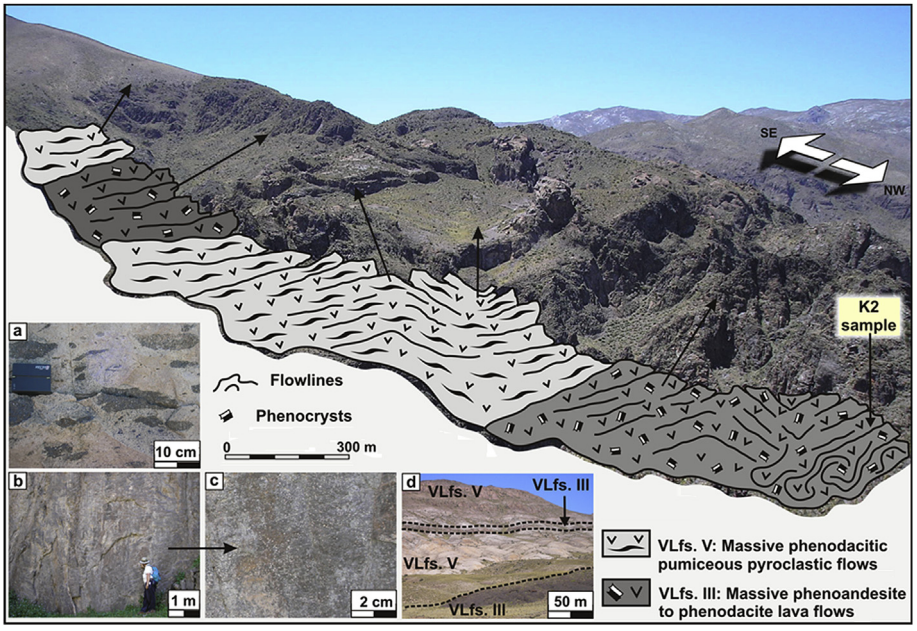

Figure 7. Quebrada Seca profile showing the location of K2 sample used for geochronological study. (a) Deformed crystals-rich andesite fragments included in the high-temperature ignimbrites; (b) flow lines in the crystal-rich andesite to dacite lava flows. K2 sample was taken in this outcrop; (c) detailed flow lines; (d) interbedding of crystal-rich andesite lava flows and massive dacitic pumiceous pyroclastic flows.

Table 4
Chemical analyses of selected samples of the Choiyoi Group lower section (major elements in wt.%, trace elements in ppm).

Sample	Basic breccias (VLfs. I)			Phenobasalts (VLfs. II)				Phenoandesites (VLfs. II)			Phenodacites (VLfs. III)			Pumiceous phenodacitic (VLfs. V)				
	V5	V13	V15	V19	V20	V31	B13	V17	M17	F15	RM2	K2	I6	F10	B21	B29	M15A	F14
SiO_2	58.11	56.76	56.17	54.05	56.51	52.31	54.64	57.39	55.96	57.92	65.42	66.22	65.32	68.63	68.38	70.30	70.27	69.17
Al_2O_3	13.44	14.70	15.89	17.82	18.18	15.02	16.77	15.11	16.30	16.08	16.02	15.94	15.42	14.28	13.16	12.48	14.72	15.24
$Fe_2O_3^T$	5.01	4.33	6.66	6.15	6.80	6.72	8.01	6.21	7.01	6.96	3.79	3.03	3.18	2.97	2.29	3.29	3.00	3.00
MnO	0.09	0.10	0.08	0.10	0.05	0.15	0.09	0.09	0.09	0.13	0.05	0.04	0.06	0.06	0.05	0.07	0.05	0.04
MgO	2.41	1.38	3.33	1.80	1.46	1.56	3.12	2.45	2.93	2.61	0.58	0.63	0.82	0.29	0.32	0.08	0.09	0.04
CaO	5.75	7.50	4.61	4.62	3.16	8.30	7.28	4.88	4.07	4.27	1.44	1.14	2.03	1.09	1.85	2.33	0.93	1.70
Na_2O	3.26	4.61	3.71	6.49	7.11	4.89	4.08	3.17	3.55	3.67	5.29	4.42	5.01	4.87	4.78	3.97	5.51	5.16
K_2O	2.50	2.21	2.22	2.63	2.35	1.94	2.42	2.66	4.16	3.42	5.09	5.00	4.66	4.68	3.99	3.62	2.31	3.85
TiO_2	0.53	0.61	0.84	0.79	0.84	0.67	1.08	0.70	1.02	1.03	0.65	0.59	0.54	0.48	0.28	0.36	0.47	0.48
P_2O_5	0.23	0.23	0.29	0.33	0.31	0.34	0.29	0.29	0.31	0.33	0.17	0.17	0.15	0.13	0.08	0.12	0.14	0.16
LOI	7.39	6.00	5.89	4.30	2.86	7.73	2.25	6.24	3.32	2.28	0.66	1.48	2.84	1.44	4.61	2.18	1.17	1.59
Total	98.74	99.22	99.68	99.08	99.63	99.63	100.00	99.18	98.73	98.70	99.16	98.65	100.00	98.90	99.79	98.81	98.64	98.65
Rb	50	21	36	35	29	31	48	46	134	117	149	148	136	118	89	53	40	87
Sr	520	679	437	878	855	646	710	503	575	684	320	379	239	273	119	126	131	148
Y	18	19	20	22	21	20	19	18	27	26	25	23	28	30	22	37	31	19
Zr	186	170	177	211	215	186	166	195	270	276	293	282	348	324	187	388	324	338
U	0.80	0.70	0.60	0.80	0.60	0.60	0.80	0.60	3.00	3.10	2.30	1.30	2.10	1.40	1.30	2.70	1.60	1.70
Nb	6.00	6.00	6.00	7.00	6.00	7.00	5.00	6.00	11.00	11.00	11.00	12.00	10.00	11.00	10.00	14.00	13.00	13.00
Ba	907	323	891	1482	1004	789	892	879	1324	840	1204	1191	1301	1241	505	842	533	884
Hf	4.60	4.10	4.30	5.00	5.10	4.50	4.40	4.40	7.60	7.60	7.40	8.00	8.60	8.40	5.40	9.90	8.50	8.70
Ta	0.30	0.20	0.30	0.30	0.30	0.30	0.30	0.30	0.70	0.70	0.70	0.80	0.70	0.80	0.80	0.90	0.70	0.80
Th	3.60	2.60	2.40	3.00	2.60	2.50	2.60	2.60	10.60	10.50	13.40	14.60	8.30	9.50	10.90	15.30	8.40	8.60
Sc	10.00	10.00	15.00	10.00	12.00	11.00	21.00	11.00	16.00	17.00	7.00	7.00	9.00	7.00	6.00	10.00	5.00	6.00
V	56	61	120	105	114	67	198	99	155	154	37	34	38	23	21	5	8	5
Cr	40.00	70.00	20.00	20.00	20.00	20.00	30.00	20.00	50.00	50.00	20.00	20.00	20.00	20.00	20.00	20.00	20.00	20.00
Co	7.00	6.00	15.00	11.00	14.00	14.00	23.00	14.00	16.00	17.00	4.00	3.00	4.00	3.00	4.00	2.00	3.00	2.00
Ga	14.00	10.00	17.00	17.00	17.00	15.00	23.00	17.00	17.00	17.00	17.00	16.00	22.00	19.00	16.00	11.00	13.00	13.00
Cs	3.10	2.20	2.00	1.80	2.00	2.70	0.90	1.50	7.50	4.80	3.60	2.10	3.70	2.30	56.60	0.50	0.80	0.50
Tl	0.20	0.10	0.20	0.10	0.10	0.10	0.10	0.40	0.40	0.30	0.50	0.40	0.30	0.40	0.50	0.30	0.20	0.10
Pb	9.00	14.00	10.00	11.00	15.00	14.00	13.00	24.00	28.00	11.00	30.00	24.00	12.00	21.00	16.00	17.00	13.00	19.00
La	31.50	24.60	27.60	33.30	31.00	28.00	26.40	27.20	33.80	33.40	35.30	33.30	44.90	44.10	43.00	43.30	36.30	43.30
Ce	59.50	48.70	54.30	64.40	60.40	54.70	56.10	53.70	73.90	73.60	75.00	72.30	90.40	90.80	82.20	103.00	79.00	91.00
Pr	7.09	6.15	6.77	7.90	7.45	7.13	7.26	6.63	8.79	8.72	8.43	8.26	10.70	10.80	9.03	11.10	8.94	10.30
Nd	27.80	25.70	27.70	31.80	30.20	29.00	28.50	26.60	34.70	34.00	32.10	30.90	39.50	38.50	30.90	42.00	33.70	38.10
Sm	5.10	5.10	5.60	6.20	5.90	5.60	5.80	5.10	6.90	6.90	6.50	5.90	7.10	6.90	5.20	8.40	6.40	6.20
Eu	1.38	1.33	1.55	1.81	1.69	1.66	1.73	1.44	1.48	1.53	1.41	1.17	1.76	1.27	1.08	1.51	1.19	1.01
Gd	4.00	4.20	4.70	5.30	5.10	4.70	5.00	4.30	6.20	6.10	5.30	4.90	5.80	5.60	3.90	7.30	5.60	4.70
Tb	0.60	0.60	0.70	0.80	0.70	0.70	0.80	0.60	0.90	0.90	0.80	0.70	1.00	1.00	0.70	1.20	0.90	0.60
Dy	3.00	3.00	3.70	3.90	3.70	3.50	4.20	3.20	5.10	4.90	4.20	4.20	5.60	5.70	4.30	6.70	5.40	3.40
Ho	0.60	0.60	0.70	0.70	0.70	0.70	0.80	0.60	1.00	1.00	0.80	0.80	1.10	1.20	0.90	1.30	1.10	0.70
Er	1.80	1.70	2.00	2.20	2.10	2.00	2.40	1.90	2.90	2.80	2.30	2.50	3.40	3.70	2.70	3.90	3.30	2.20
Tm	0.28	0.24	0.29	0.32	0.31	0.30	0.34	0.27	0.42	0.41	0.34	0.36	0.51	0.56	0.44	0.59	0.49	0.35
Yb	1.80	1.50	1.80	2.00	2.00	1.90	2.10	1.70	2.70	2.60	2.10	2.30	3.40	3.60	3.00	4.00	3.10	2.50
Lu	0.28	0.22	0.26	0.30	0.30	0.29	0.31	0.26	0.41	0.39	0.31	0.35	0.50	0.56	0.47	0.63	0.48	0.40

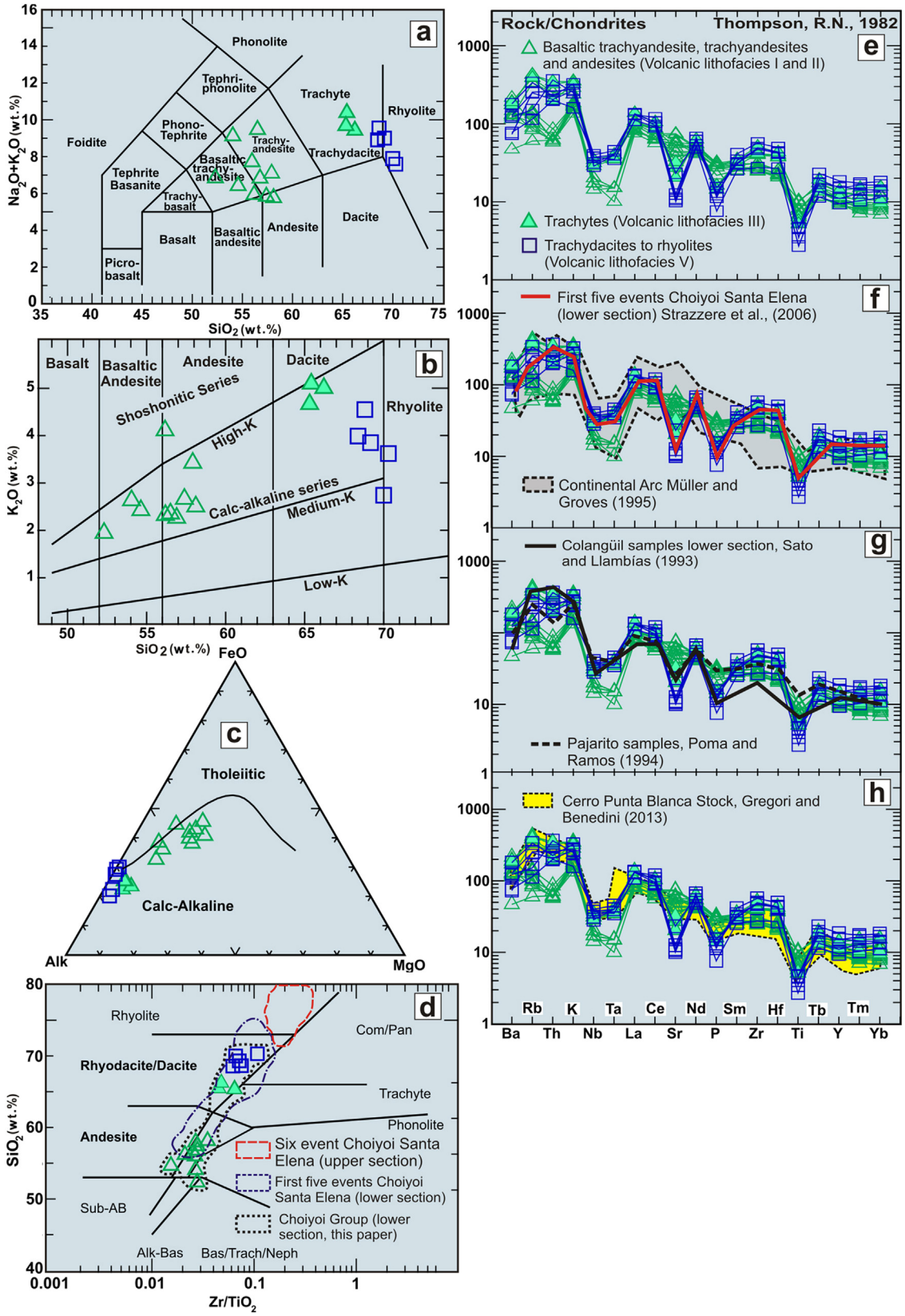

Figure 8. Geochemical compositions (a) classification of the samples in the Le Maitre et al. (1989) diagram; (b) classification of volcanic rocks in Pecerrillo and Taylor's (1976) diagram; (c) the calc-alkaline trend displayed in Irvine and Baragar (1971) diagram; (d) classification of volcanic rocks in Winchester and Floyd (1977) diagram. Dotted lines fields were constructed using Strazzere et al. (2006) data for the first five events and the sixth of the Choiyoi Group in the Quebrada de Santa Elena and Telégrafo; (e) expanded trace elements diagram (Thompson, 1982) of volcanic rocks; (f) expanded trace elements diagram (Thompson, 1982). The fill red line represents the first five events in the Quebrada de Santa Elena and Telégrafo studied for Strazzere et al. (2006). Dotted line field represents chondrite-normalized spidergram patterns for potassic igneous rocks from a continental arc setting constructed by Müller and Groves (1995); (g) expanded trace elements diagram (Thompson, 1982). The samples are compared with data from Sato and Llambías (1993) (black fill line) and Poma and Ramos (1994) data (black tip line); (h) expanded trace elements diagram (Thompson, 1982). Samples are compared with Cerro Punta Blanca data from Gregori and Benedini (2013) (yellow tip line field).

Table 5
Geochronological analyses of sample K-2, Choiyoi Group lower section.

Analysis	U-Pb geochronological analyses					Isotope ratios					Apparent ages (Ma)						
	U (ppm)	$^{206}Pb/^{204}Pb$	U/Th	$^{206}Pb^*/^{207}Pb^*$	± (%)	$^{207}Pb^*/^{235}U^*$	± (%)	$^{206}Pb^*/^{238}U$	± (%)	Error corr.	$^{206}Pb^*/^{238}U^*$	± (Ma)	$^{207}Pb^*/^{235}U$	± (Ma)	$^{206}Pb^*/^{207}Pb^*$	± (Ma)	Best age (Ma)	± (Ma)
K2-5	132	646	1.0	22.240	7.6	0.289	7.6	0.047	1.0	0.13	293.4	2.9	257.5	17.4	−57.5	184.5	293.4	2.9
K2-8	435	4664	1.6	18.553	2.3	0.328	3.5	0.044	2.6	0.75	278.4	7.2	288.0	8.8	366.8	52.1	278.4	7.2
K2-9	127	1244	1.3	18.125	6.8	0.332	6.8	0.044	1.0	0.15	275.5	2.7	291.3	17.3	419.2	151.1	275.5	2.7
K2-10	108	826	0.7	19.685	7.0	0.323	7.2	0.046	1.5	0.20	290.5	4.1	284.1	17.8	231.8	162.9	290.5	4.1
K2-14	196	1606	1.0	17.218	6.2	0.363	6.3	0.045	1.0	0.16	285.7	2.8	314.3	17.0	532.7	136.1	285.7	2.8
K2-15A	80	406	1.2	20.812	20.6	0.281	20.6	0.042	3.3	0.16	267.6	8.7	251.3	46.6	101.7	492.5	267.6	8.7
K2-18	144	2856	1.5	17.975	9.2	0.336	9.4	0.044	1.5	0.16	276.5	4.2	294.3	23.9	437.8	206.1	276.5	4.2
K2-22	201	4604	2.1	19.431	3.8	0.301	4.1	0.042	1.6	0.38	268.0	4.1	267.3	9.6	261.7	87.0	268.0	4.1
K2-23	192	1106	1.8	16.749	8.4	0.358	9.0	0.043	3.5	0.38	274.3	9.3	310.6	24.2	592.9	181.4	274.3	9.3
K2-23A	106	672	1.4	18.703	11.8	0.316	12.0	0.043	2.1	0.18	270.9	5.6	279.2	29.2	348.7	267.2	270.9	5.6
K2-24	63	2056	1.6	19.815	8.5	0.304	9.0	0.044	3.1	0.34	276.0	8.3	269.9	21.4	216.5	196.7	276.0	8.3
K2-25	95	1642	1.3	16.977	3.4	0.357	4.2	0.044	2.4	0.58	277.2	6.5	309.9	11.2	563.5	74.6	277.2	6.5
K2-26	37	1048	1.9	20.430	6.1	0.311	6.4	0.046	1.9	0.29	290.4	5.3	274.9	15.4	145.3	143.9	290.4	5.3
K2-26A	36	984	1.7	19.499	11.7	0.308	11.8	0.044	1.4	0.12	275.2	3.7	272.9	28.3	253.6	270.9	275.2	3.7
K2-27	47	940	2.2	19.249	8.4	0.328	8.5	0.046	1.0	0.12	288.4	2.9	287.9	21.3	283.2	193.6	288.4	2.9
K2-28	176	1964	1.2	17.565	5.2	0.346	6.0	0.044	3.0	0.49	277.8	8.1	301.4	15.7	488.8	115.5	277.8	8.1
K2-29	146	3888	1.8	18.102	6.6	0.330	6.8	0.043	1.6	0.23	273.4	4.3	289.5	17.2	422.1	147.9	273.4	4.3
K2-30A	230	1374	0.9	20.133	3.7	0.305	3.8	0.045	1.0	0.26	280.9	2.7	270.3	9.1	179.5	86.6	280.9	2.7
K2-31	275	1442	0.8	20.200	9.1	0.298	9.3	0.044	2.0	0.22	275.9	5.5	265.2	21.8	171.8	213.2	275.9	5.5

Both TAS diagram of Le Maitre et al. (1989; Fig. 8a) and AFM diagram of Irvine and Baragar (1971; Fig. 8c) display a small gap between volcanic lithofacies I and II and volcanic lithofacies III and V.

The $Mg^{\#}$ ranges from 18 to 33 for VLfs. I and II, between 13 and 20 for VLfs. III, and 1.32 to 12 for VLfs. V displaying a decreasing of $Mg^{\#}$ with increasing of SiO_2.

4.2. Trace elements

According to the Zr/TiO_2 versus SiO_2 diagram (Winchester and Floyd, 1977, Fig. 8d) the samples fall in the andesite field (VLfs. I and II) and dacite to rhyodacite fields for VLfs. III and V (Fig. 8d). If samples from Quebrada de Santa Elena (Strazzere et al., 2006) are also plotted, a continuous trend from andesite to rhyolite can be observed.

In the study area andesitic rocks are more common that in Quebrada de Santa Elena, where all the samples are subduction-related (Strazzere et al., 2006). The sixth event described in Quebrada de Santa Elena, Strazzere et al. (2006) is not represented in the study area.

The SiO_2 versus Sr or Ba diagrams show a negative correlation due to plagioclase fractionation (not shown).

The spider diagrams (Fig. 8e–h) of trace elements and REE have been normalized to chondrite (Thompson, 1982) and display positive anomalies in LILE and strong negative Nb and Ta. The basaltic trachyandesites, trachyandesites and andesites suites show strong negative Nb and Ta anomalies and enrichment in Sr, P and Ti that the trachytes and trachydacites to rhyolite group (Fig. 8e).

Samples are similar (Fig. 8f) to those of continental arc rocks of Müller and Groves (1995). Trachytes (VLfs. III), trachydacites to rhyolites (VLfs. V) are coincident with the first five events from Quebrada de Santa Elena (Strazzere et al., 2006) whereas basaltic trachyandesites, trachyandesites and andesites (VLfs. I and II) are the less evolved rocks of the sequence.

When compared with samples of the Choiyoi Lower section from Cordón de Colangüil (Sato and Llambías, 1993) and Cerro Pajarito (Poma and Ramos, 1994), the trachytes and trachydacites to rhyolites display a similar trend, but the basaltic trachyandesites, trachyandesites and andesites show more negative Nb, Ta, and Th anomalies (Fig. 8f).

If samples of the Cerro Punta Blanca from Cordon del Portillo are compared (Gregori and Benedini, 2013), the basaltic trachyandesites, trachyandesites, and andesites show a bigger negative Nb–Ta anomaly meaning a major subduction component that the granites.

4.3. Rare earths

The chondrite-normalized diagrams (Sun and McDonough, 1989) show (Fig. 9a) that samples are 100–200 times enriched in light REE and 10 to 30 times in heavy REE respect to chondrite. There is an ongoing evolution from basaltic trachyandesites towards rhyolites where the first suite is less enriched in light and heavy rare earths.

The Eu anomaly is absent in the more basic suite but notable in the acidic facies. In order to compare samples of the studied area with the six events of the Choiyoi Group recognized at Quebrada de Santa Elena and del Telégrafo dashed fields (Fig. 9b) were built with data from Strazzere et al. (2006). Samples that match the first five events are the less enriched and less evolved members of basaltic trachyandesitic composition.

The basaltic trachyandesites are comparable to samples of the Cerro Punta Blanca Stock of Gregori and Benedini (2013), while trachytes to rhyolites fit better with Cerro Bayo Stock of Gregori and Benedini (2013; Fig. 9c, d).

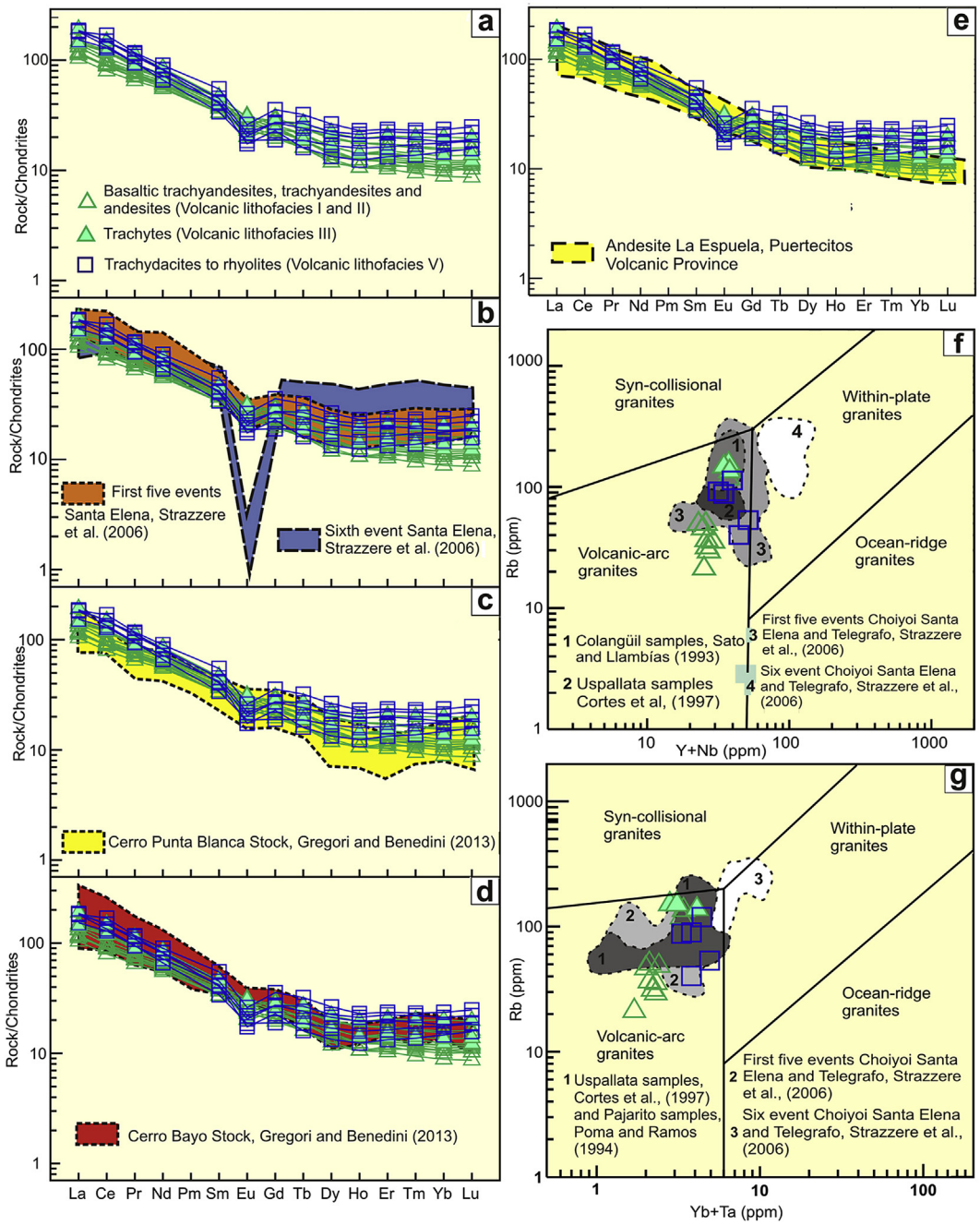

Figure 9. (a) Chondrite-normalized to Sun and McDonough (1989) spider diagram of volcanic rocks. (b) Chondrite-normalized to Sun and McDonough (1989) spider. Dotted field represents the first five events and the sixth of the Choiyoi Group in the Quebrada del Santa Elena and Telégrafo from Strazzere et al. (2006). (c) Chondrite-normalized to Sun and McDonough (1989) spider diagram. Dotted field represents the Cerro Punta Blanca from Gregori and Benedini (2013). (d) Chondrite-normalized to Sun and McDonough (1989) spider diagram. Dotted field represents the Cerro Bayo Stock from Gregori and Benedini (2013). (e) Chondrite-normalized to Sun and McDonough (1989) spider diagram. Dotted field represents andesite La Espuela from Mora-Klepeis and Mc Dowell (2004). (f) Rb vs. Y+Nb diagram (Pearce et al., 1984) showing evolution from volcanic arc granite to within-plate granite. Dotted field represents: (1) Colangüil samples from Sato and Llambías (1993), (2) Uspallata samples from Cortés et al. (1997), (3, 4) first five events and the sixth event of the Choiyoi Group in the Quebrada del Santa Elena and Telégrafo from Strazzere et al. (2006). (g) Rb vs. Y+Ta diagram (Pearce et al., 1984) showing evolution from volcanic arc granite to within-plate granite. Dotted field represents: (1) Uspallata and Pajarito samples, (2, 3) first five events and the sixth event of the Choiyoi Group in the Quebrada del Santa Elena and Telégrafo.

Patterns of La Espuela andesite (Mora-Klepeis and McDowell, 2004) located in the northwest of Mexico, which represent the first stage of development of a magmatic arc on continental crust, are indiscernible from the basaltic trachyandesites, trachyandesites and dacites (VLfs. I and II, Fig. 9e). Trachytes, trachydacites and rhyolites are more evolved when compared to La Espuela andesite (Fig. 9e).

5. Geotectonic setting of the Portezuelo del Cenizo Formation

In the Yb+Nb vs. Rb diagram of Pearce et al. (1984) of Fig. 9f, the dashed fields were built with data from Cordón de Colangüil (Sato and Llambías,1993), Uspallata area (Cortés et al., 1997) and Quebrada de Santa Elena and del Telégrafo (Strazzere et al., 2006). The samples of Cordón de Colangüil show magmatic arc affinities, while

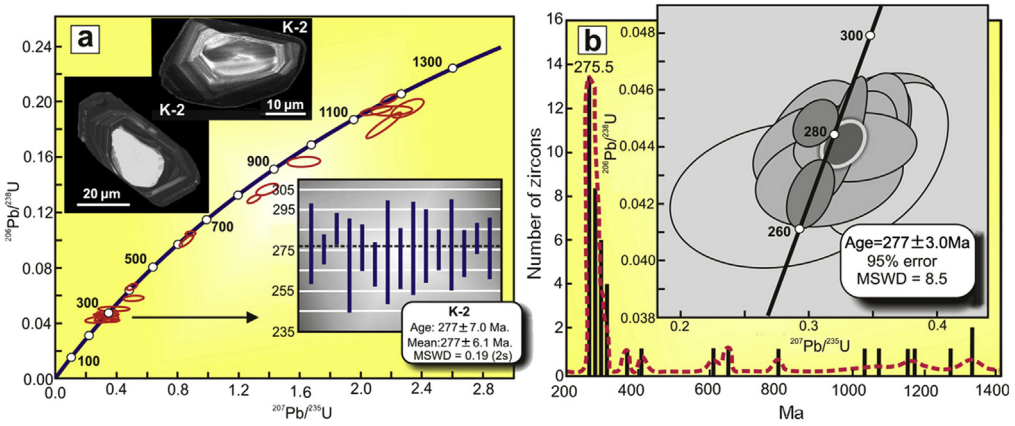

Figure 10. U-Pb dating in zircon from sample K-2 of the Choiyoi Group lower section (Portezuelo del Cenizo Formation). (a) Upper insert show zoned zircon of K-2 sample. Main diagram displays the $^{207}Pb/^{235}U$ vs. $^{206}Pb/^{238}U$ concordia diagram. Lower insert shows the mean weight age diagram for K-2 sample. (b) Main diagram shows the U-Pb zircon provenance age pattern. The curves in the diagram are relative probability trends based on the preferred age derived from individual measurements, which are also shown. The insert is a detail of the concordia diagram of (a).

those from Uspallata area show a trend from arc magmatism, in the first five events to intraplate in the last one (sixth event). The samples here studied plot close to those of the Uspallata area (Strazzere et al., 2006), and displayed magmatic arc affinities (Fig. 9f).

The same results are obtained considering the Yb+Ta vs. Rb diagram (Fig. 9g) of Pearce et al. (1984), where the samples from Uspallata area (Cortés et al., 1997) and Choiyoi Lower section at Cerro Pajarito, Cordón del Portillo (Poma and Ramos, 1994) were included.

6. Age of the Portezuelo del Cenizo Formation

Within the lithofacies recognized in the Portezuelo del Cenizo Formation, the trachydacites have the largest number of zircon crystals, and since they appear in a relatively low position in the sequence, these rocks were selected for the geochronological study. Sample K2 comes from the Quebrada Seca profile (Figs. 2 and 7), corresponds to a massive phenoandesite to phenodacite lava-flow 1–2 m thick. Scarce, non-vesiculated juvenile fragments of phenoandesite were recognized. Under microscope, porphyritic to trachytic texture with plagioclase, amphibole, pyroxene phenocrysts and a glassy groundmass were identified. Amphibole and pyroxene are replaced.

Zircons were separated after crushing, using heavy liquids and magnetic separator and concentration by hand panning. Microphotography in transmitted and reflected light, shows euhedral crystals of zircon with sizes varying between 30 and 40 µm (Fig. 10a). Their internal zoning was detected by cathodoluminescence (CL) using scanning electron microscope (Fig. 10a).

The sample was analyzed using the U-Th-Pb technique on zircon at the LaserChron Center, Arizona. A Laser – Ablation Multicollector ICP Mass Spectrometer was used for the detection of these elements, following the procedures described by Gehrels et al. (2008). The results are displayed in Table 5.

The age obtained for the trachydacite is 277 ± 3.0 Ma (Fig. 10) yielding a lower Permian (Kungurian) age.

Therefore, the trachyandesites and trachybasalts, as well as, the Conglomerado del Río Blanco, which are located lower in the sequence must have older ages.

Rocks with similar age were described by Barrionuevo et al. (2013) at Cerro Colón (La Pampa Province) where four U-Pb single zircon ages average 261 Ma. Barrionuevo et al. (2013) interpreted these ages as belonging to the Upper Section of Choiyoi Group. Also in La Pampa Province, in isolated outcrops of rhyolitic rocks Domeier et al. (2011) get U/Pb ages in zircon of 268, 263 and 257 Ma, possibly related to the Choiyoi Group volcanism.

In the eastern part of the Domeyko Cordillera, northern Chile, the La Tabla Formation consists of a 800 m thick succession formed of rhyolites, rhyolitic tuffs, breccias, and basaltic intercalations (without exposed base). U-Pb in zircon of banded rhyolites and rhyolitic tuff yield ages from 282.0 ± 11.4 to 270.4 ± 4.6 Ma (Maksaev et al., 2014).

7. Discussion

7.1. The marine basement of the Choiyoi Lower section

In the Precordillera and Cordillera Frontal area, the upper Carboniferous and lower Permian are represented by marine and continental basins. The marine Calingasta-Uspallata sub-basin covers part of the Precordillera and Cordillera Frontal of San Juan and Mendoza provinces.

The Santa Elena Group of the Precordillera is considered upper Carboniferous and lower Permian (Archangelsky and Lech, 1985) due to the presence of *Cancrinella* sp., typical of lower Permian age. In the El Plata and Loma de Los Morteritos formations of Cordillera Frontal, the presence of *Lissochonetes* sp., *Cancrinella* sp., *Neospirifer* sp., *Spirifer* sp. and *Orbiculoidea* sp. (Aparicio, 1966) allows to assign an upper Carboniferous age for the sedimentation. The upper sections of these units could have similar ages to the continental units developed in the Paganzo Basin, locates eastwards. Radiometric dating made in basaltic lava-flows within this continental sequences exhibit ages of 292 ± 6 and 295 ± 6 Ma (Thompson and Mitchell, 1972).

In the El Plata Formation, Gregori et al. (1996) recognized subvolcanic bodies of EMORB composition, which suggest the expansion of an incipient oceanic crust during the development of the marine basins in the Cordillera Frontal. This evidence suggests a back-arc setting during the deposition of the marine units.

Possible evidence of the occurrence of a magmatic arc located westwards could be the boulders of granitoids and altered volcanic rocks that make up the conglomerate levels of the lower section of the Las Peñas Formation, identified by Polanski (1958). Mpodozis and Kay (1992), Parada Velazquez (2013) and Hervé et al. (2014) described arcs of this age in the Elqui-Limari area (Chile).

The closure of the marine basin, together with its rising and deformation should have happened in a relatively short time

(Gregori and Benedini, 2013). This deformation is known as San Rafael diastrophic phase (Polanski, 1958).

7.2. Timing of the San Rafael diastrophic phase and closure of the marine basin

In the Cordillera Frontal of Chile the magmatic activity of Elqui-Limari Complex ends with the intrusion of the Montosa and El Volcán plutons that were related to pre- and syn-collisional stages during the subduction vanishing.

Mpodozis and Kay (1992) associated the change in the continental crust thickness during upper Carboniferous with the deformation due to the San Rafael diastrophic phase.

The age of the deformation is located between 265 and 270 Ma according to Azcuy and Caminos (1987) or prior to 252 Ma (Ramos, 1988). For Mpodozis and Kay (1992) the rise of the Cordillera Frontal of Chile or the accretion of the X terrane occurs between 260 and 242 Ma.

In the Cordón de Colangüil, Llambías and Sato (1995) interpreted that the San Rafael diastrophic phase would extend for about 10 Ma, from 272 to 280 Ma, being 30 Ma older than the rise-collision event in the Cordillera Frontal of Chile.

The U/Pb age obtained in the Quebrada Seca, indicates that the first effusions of the Choiyoi Group took place prior to 277 ± 3.0 Ma. Therefore, the San Rafael diastrophic phase is not longer than 5 Ma being comprised between 285 and 290 Ma, probably Artinskian (lower Permian). This age is consistent with the ideas of Llambías and Sato (1995).

The San Rafael diastrophic phase seems to be related to a slight decrease in the angle of the subduction plane located westwards. This fact increased the horizontal coupling between both crusts, resulting in a dominant tangential deformation in the foreland area with the consequent uplifting of the continental crust and the retreat of the upper Carboniferous Sea.

The progressive deformation produced the disappearance of the marine basin, E-vergent folding, thrusting, and uplift along a N–S orogenic corridor in the Cordillera Frontal and Precordillera.

However, these deformed sequences exhibit also NW–SE and NNE–SSW structures associated with oblique-strike displacement during deformation. The presence of foliated protoclastic and cataclastic textures, as well as, mylonitic belts in the younger stock of the Elqui-Limari Complex (Mpodozis and Kay, 1992) are evidence of a possible change in the angle of convergence associated to along-strike deformation.

Once the San Rafael diastrophic phase decreasing, the mountain chain undergone an extensional tectonic regime. The period of erosion appears to be short in time since the surface of erosion shows small relief, at least in the studied area, where the Conglomerado del Río Blanco is only 100 m thick.

The outcrops of the Conglomerado del Río Blanco show a similar, sub-parallel design that mimetic major structures of the deformed marine sequences, indicative that the developed of these depocenters were conditioned by the structural style of the marine sequences deformed during the San Rafael diastrophic phase.

The same applies for the outcrops of the Portezuelo del Cenizo Formation, that have a similar design of the post-San Rafael diastrophic phase depocenters, suggesting that the development of the volcanic system follows structural lineaments generated during the deformation of the marine sequences.

7.3. The relationship with the Carboniferous marine sequences

Several authors have described the relationships between the upper Carboniferous and lower Permian marine sequences and the Choiyoi Group.

In the Precordillera of Mendoza, Harrington (1941) described the Conglomerado de Las Pircas at Mogote de Las Pircas (Fig. 1i), whereas near Cerro La Cantera, Pöthe de Baldis (1975) identified a conglomerate located at the base of the Choiyoi Group (Fig. 1g).

In the Cordillera Frontal of Mendoza Province, Fernández (1955) studied, west of Portezuelo Santa Clara, near Río Tupungato, a red purple to blue purple conglomerate, considered as alluvial fans, located on angular unconformity over the upper Paleozoic sequences (Fig. 1k).

González Díaz (1957) recognized on the northeastern side of Cordón del Portillo, the Portezuelo Ancho Formation, composed of basic and acidic volcanic rocks, as well as, alluvial conglomerates. The rocks are in non-concordance over the upper Carboniferous and lower Permian marine sequences. The author considered the sequence as late Carboniferous–Permian (Fig. 1j).

On the east side of the Cordón del Tigre, Coira and Koukharsky (1976) described a conglomerate, located on angular unconformity over Neopaleozoic marine sequences (Fig. 1e). The authors used the name of Portezuelo del Cenizo for breccias, tuff and lava flows of andesitic and dacitic composition, considered as the first volcanic event.

In Estancia Tambillos, Cordón del Tigre, Cortés (1985) described a volcanic sequence composed by ignimbrites interbedded with pyroclastic and lacustrine deposits (Fig. 1f). Cortés (1985) considered these deposits as the base of the Choiyoi Group, located unconformably over Devonian and Carboniferous marine sequence.

In the Cordón de Colangüil, San Juan Province, Sato and Llambías (1993) assigned 300 m of conglomerates, sandstones, and pelites to the base of Choiyoi Group, which rest unconformable on Neopaleozoic marine sequences (Fig. 1a).

In the Cordillera Frontal of San Juan Province, west of Calingasta, Caballé (1990) recognized two sequences of progressive acidification (Fig. 1c). Heredia et al. (2002) in the Cordillera de La Totora, documented a lower section of Choiyoi Group constituted by tuff, volcanic agglomerates, ignimbrites, epiclastic rocks and calcareous mudstones (Fig. 1b).

In the above-mentioned areas, the stratigraphic schema shows similarities respect to the relationships between the Choiyoi Group and the Neopaleozoic marine sequences. The San Rafael diastrophic phase deformed the marine sequence and produces an irregular relief where shallow continental depocenters were emplaced. In these appear conglomerates and sedimentary sequences typical of proximal alluvial fans, which transitionally pass to fluvial and lacustrine environments. The first basic volcanic event is interbedded and is coeval with the sedimentary sequence.

7.4. Chemical constrains

As indicated in section 4, the comparison of the chemical data presented by Sato and Llambías (1993), Cortés et al. (1997) and Strazzere et al. (2006) in the Yb+Nb vs. Rb diagram of Pearce et al. (1984) for the Portezuelo del Cenizo Formation shows that basaltic trachyandesites, trachyandesites and andesites display subduction-zone signature. The trachytes, trachydacites and rhyolites show a trend from magmatism arc, in the early events to intraplate magmatism in the late ones (Fig. 9f).

The trachytes, trachydacites, and rhyolites are coincident with the first five events of Strazzere et al. (2006) and with the Choiyoi Upper section at Cordón de Colangüil. The presence of ignimbrites interbedded on block and ash lava-flows of the Portezuelo del Cenizo Formation in the studied area show that acidic volcanism was coeval with the development of intermediate-basic magmatism.

After the 277 Ma event occurs a considerable expansion of the Choiyoi Group volcanism with a notable increasing of its thickness,

energy and dispersion of the deposits (Strazzere et al., 2006). The geochemistry of this volcanism indicates progressive changes in the composition of the magma from basaltic-andesitic to rhyolitic. The magmatism is mostly high-K calk-alkaline.

Harker diagrams and others show that these rocks are linked each another through fractionated crystallization. Traces element diagrams (Pearce et al., 1984) suggest a significant decrease in subduction components along evolution. There is a clear transition from rocks generated in volcanic-arcs to those generated in intra-plate environments under extensional conditions.

8. Conclusion

In the eastern side of the Cordón del Plata and the western side of Precordillera of Mendoza, the Conglomerado del Río Blanco and the Portezuelo del Cenizo Formation, lower part of the Choiyoi Group rests on significant irregular topography over the upper Carboniferous–lower Permian marine sedimentary sequences.

Six lithofacies and three facies associations were recognized in the Conglomerado del Río Blanco. Depositional mechanism was mantled and gravitational flows modified by high-energy fluvial currents that evolved to low-energy fluvial and lacustrine environments. Several, minor reactivation cycles were observed along the sequence.

Volcanic breccias and scarce lava-flows of the Portezuelo del Cenizo Formation interbedded in the Conglomerado del Río Blanco, suggest that both units are transitional and partly coeval.

Five lithofacies and three volcanic associations were recognized in the Portezuelo del Cenizo Formation. The first volcanic event in the Portezuelo del Cenizo Formation is lava-flows of basaltic to andesitic composition emplaced in the flanks of volcanoes. Posterior collapse produced thick block and ash flows. Geochemistry of these rocks induces to consider they belong to a magmatic arc on continental crust, considered the less evolved event in the Choiyoi Group evolution.

The age of the Portezuelo el Cenizo Formation is Kungurian (277 ± 3 Ma, late lower Permian) which is coincident with the first magmatic event recognized by Gregori and Benedini (2013) in the Cordón del Portillo, Mendoza Province.

Therefore, the age of the San Rafael Orogenic phase at the studied area should be older than 277 Ma, like in the Cordón del Portillo, restricting the time for the San Rafael diastrophic phase to the Artinskian.

Acknowledgments

Financial support to D. Gregori was provided by the Universidad Nacional del Sur and CONICET (project 21H121) for the study of the Gondwanan magmatism of the Cordillera Frontal. We are also greatly indebted to Mercedes Barros (Cátedra de Geología Argentina, UNS) for assistance provided during fieldtrips and discussions of Gondwanan magmatism. Constructive and thoughtful reviews by two anonymous colleagues and the editor on the early version greatly improved the same and are truly thanked.

References

Aparicio, E.P., 1966. Sobre el hallazgo del yacimiento fosilífero de Agua de las Cortaderas y su posición estratigráfica. Revista de la Asociación Geológica Argentina 21 (3), 190–193.

Archangelsky, A., Lech, R., 1985. Presencia de *Cancrinella aff. Ferleyensis* (Eth y Dunn) en las capas plegadas de la <<Serie Tramojo>>, en el Pérmico Inferior de la Precordillera de Mendoza, Argentina. 1° Jornadas de Geología de Precordillera (San Juan, 1985) 1, 187–191.

Azcuy, C.L., 1993. Las secuencias sedimentarias neopaleozoicas. In: Ramos, V.A. (Ed.), Geología y Recursos Naturales de Mendoza. XII Congreso Geológico Argentino y II Congreso Exploración de Hidrocarburos, Relatorio I (5), 41–52.

Azcuy, C.L., Caminos, R., 1987. Diastrofismo. In: Archangelsky, S. (Ed.), El Sistema Carbonífero en la República Argentina. Academia Nacional de Ciencias Córdoba, Córdoba, pp. 239–251.

Azcuy, C.L., Carrizo, H.A., Caminos, R., 1999. Carbonífero y Pérmico de las Sierras Pampeanas, Famatina, Precordillera, Cordillera Frontal y Bloque de San Rafael. In: Caminos, R. (Ed.), Geología Argentina, Servicio Geológico Minero Argentino, Anales, vol. 29, pp. 261–318 (Buenos Aires).

Barredo, S., Chemale, F., Marsicano, C., Ávila, J.N., Ottone, E.G., Ramos, V.A., 2012. Tectono-sequence stratigraphy and U–Pb zircon ages of the Rincón Blanco Depocenter, northern Cuyo Rift, Argentina. Gondwana Research 21, 624–636.

Barrionuevo, M., Arnosio, M., Llambías, E.J., 2013. Nuevos datos geocronológicos en subsuelo y afloramientos del Grupo Choiyoi en el oeste de La Pampa: implicancias estratigráficas. Revista de la Asociación Geológica 70 (1), 31–39.

Borrello, A.V., 1969. Embriotectónica y tectónica tensional. Su importancia en la evolución estructural de la Precordillera. Revista de la Asociación Geológica Argentina XXIV (1) (Buenos Aires).

Caballé, M.F., 1990. Magmatismo Permo-Triásico al oeste de Calingasta, Cordillera Frontal de San Juan, Argentina. XI Congreso Geológico Argentino Actas I, 28–31.

Caminos, R., 1965. Geología de la vertiente oriental del Cordón del Plata, Cordillera Frontal de Mendoza. Revista de la Asociación Geológica Argentina 22 (3), 351–392.

Cas, R.A.F., Wright, J.V., 1993. Volcanic Successions, Modern and Ancient. Chapman and Hall, London, 528 pp.

Coira, B., Koukharsky, M., 1976. Efusividad tardío hercínica en el borde oriental de la Cordillera Frontal, zona Arroyo del Tigre, provincia de Mendoza, República Argentina. I Congreso Geológico Chileno Actas II, F, 105–124 (Santiago).

Cortés, J.M., 1985. Vulcanitas y sedimentitas lacustres en la base del grupo Choiyoi al sur de Estancia Tambillos, Mendoza, Argentina. IV Congreso Geológico Chileno Actas I, 89–108 (Antofagasta).

Cortés, J.M., González Bonorino, G., Koukharsky, M.M.L., Pereyra, F., Brodtkorb, M., 1997. Hoja geológica 3369–09, Uspallata, provincia de Mendoza, Argentina. Subsecretaría de Minería de la Nación. SEGEMAR, 116 pp. (Buenos Aires).

Cuerda, A.J., 1988. Investigaciones estratigráficas en el "Grupo Villavicencio" Precordillera de Mendoza y San Juan, República Argentina. 5 Congreso Geológico Chileno Actas 2 (C), 177–187.

Domeier, M., Van der Voo, R., Tohver, E., Tomezzoli, R., Vizan, N.H., Torsvik, T.H., Kirshner, J., 2011. New Late Permian paleomagnetic data from Argentina: Refinement of the apparent polar wander path of Gondwana. Geochemistry, Geophysics, Geosystems 12, Q07002. http://dx.doi.org/10.1029/2011GC003616.

Fernández, P.C., 1955. Geología del Alto Río Tupungato. Revista de la Asociación Geológica Argentina 10 (2), 100–126 (Buenos Aires).

Folguera, A., Etcheverría, M., Pazos, P., Giambiagi, L., Cortes, J., Fauque, L., Rodríguez, M.F., Irigoyen, V., Fusari, C., 2004. Memoria de la Hoja Geológica 3369-15, Potrerillos, provincia de Mendoza, Argentina. Subsecretaría de Minería de la Nación. SEGEMAR, 141 pp. (Buenos Aires).

Francis, P.W., Roobol, M.J., Walker, G.P.L., Cobbold, P.R., Coward, M., 1974. The San Pedro and San Pablo volcanoes of northern Chile and their hot avalanche deposits. Geologische Rundschau 63, 357–388.

Gehrels, G.E., Valencia, V., Ruiz, J., 2008. Enhanced precision, accuracy, efficiency and spatial resolution of U-Pb ages by laser ablation-multicollector-inductively coupled plasma-mass spectrometry. Geochemistry, Geophysics, Geosystems 9, Q03017. http://dx.doi.org/10.1029/2007GC001805.

Giambiagi, L., Martinez, A.N., 2008. Permo-Triassic oblique extension in the Potrerillos-Uspallata area, western Argentina. Journal of South American Earth Sciences 26, 252–260.

González Díaz, E.F., 1957. Estructuras del basamento y del Neopaleozoico en los contrafuertes nord-orientales del Cordón del Portillo, provincia de Mendoza. Revista de la Asociación Geológica Argentina 12 (2), 98–133 (Buenos Aires).

Gregori, D., Benedini, L., 2013. The Cordon del Portillo Permian magmatism, Mendoza, Argentina, plutonic and volcanic sequences at the western margin of Gondwana. Journal of South American Earth Sciences 42, 61–73.

Gregori, D.A., Fernández-Turiel, J.L., López-Soler, A., Petford, N., 1996. Geochemistry of upper Palaeozoic-lower triassic granitoids of the Central frontal cordillera (33°10′–33°45′S), Argentina. Journal of South American Earth Sciences 9, 141–151.

Gregori, D.A., Martinez, J.C., Benedini, L., 2013. The Gondwana-South America Iapetus margin evolution as recorded by Lower Paleozoic units of western Precordillera, Argentina: the Bonilla Complex, Uspallata. instituto Superior de Correlación Geológica. Serie Correlación Geológica 29 (1), 21–80.

Groeber, P., 1946. Observaciones geológicas a lo largo del meridiano 70°. 1, Hoja Chos Malal. Revista de la Sociedad Geológica Argentina I(3), 117–208. Reprint in Asociación Geológica Argentina, Serie C. Reimpresiones 1 (1980), 1–174 (Buenos Aires).

Groeber, P., 1951. La Alta Cordillera entre las latitudes 34° y 29°30′. Instituto de Investigaciones de las Ciencias Naturales. Museo Argentino de Ciencias Naturales Bernardino Rivadavia, Revista (Ciencias Geológicas) I (5), 1-352, (Buenos Aires).

Harrington, H.J., 1941. Investigaciones geológicas en las Sierras de Villavicencio y Mal País, provincia de Mendoza. Dirección Nacional de Geología y Minería, Boletín, 49, 54 pp., Buenos Aires.

Heredia, S., 1990. Geología de la Cuchuilla del Cerro Pelado, Precordillera de Mendoza, Argentina. 11 Congreso Geológico Argentino Actas 2, 101–104.

Heredia, S., 1996. El Cámbrico y Ordovícico de la Cuchilla del Cerro Pelado, Precordillera de Mendoza, Argentina. 13 Congreso Geológico Argentino Actas 1, 591–600.

Heredia, N., Rodríguez Fernández, L.R., Gallastegui, G., Busquets, P., Colombo, F., 2002. Geological setting of the Argentina Frontal Cordillera in the flat-slab segment (30° 00'-31° 30'S latitude). Journal of South American Earth Science 15, 79–99.

Hervé, F., Fanning, M., Calderón, M., Mpodozis, C., 2014. Early Permian to Late Triassic batholiths of the Chilean Frontal Cordillera (28°–31°S): SHRIMP U–Pb zircon ages and Lu–Hf and O isotope systematics. Lithos 184–187, 436–446.

Irvine, T.N., Baragar, W.R.A., 1971. A guide to the chemical classification of the common rocks. Canadian Journal of Earth Sciences 8, 523–548.

Kay, S.M., Ramos, V.A., Mpodozis, C., Sruoga, P., 1989. Late Paleozoic to Jurassic silicic magmatism at the Gondwanaland margin: analogy to the Middle Proterozoic in North America? Geology 17, 324–328.

Kleiman, L.E., Japas, M.S., 2009. The Choiyoi volcanic province at 34°S-36° S (San Rafael, Mendoza, Argentina): implications for the Late Palaeozoic evolution of the southwestern margin of Gondwana. Tectonophysics 473, 283–299.

Kury, W., 1993. Características composicionales de la Formación Villavicencio, Devónico, Precordillera de Mendoza. XI Congreso Geológico Argentino y II Congreso de Exploración de Hidrocarburos 1, 321–328 (Mendoza, Argentina).

Le Maitre, R.W., Bateman, P., Dudek, A., Keller, J., Lameyre, J., Le Bas, M.J., Sabine, P.A., Schmid, R., Sorensen, H., Strekeisen, A., Woolley, A.R., Zanettin, B., 1989. A Classification of Igneous Rocks and Glossary of Terms. Blackwell, Oxford, 193 pp.

Llambías, E.J., Sato, A.M., 1990. El Batolito de Colangüil, Cordillera Frontal, Argentina: Estructura y marco tectónico. Revista Geológica de Chile 17 (1), 89–108 (Santiago).

Llambías, E.J., Sato, A.M., 1995. El Batolito de Colangüil: transición entre orogénesis y anorogénesis. Revista de la Asociación Geológica Argentina 50 (1–4), 111–131.

Llambias, E.J., Kleiman, L.E., Salvarredi, J.A., 1993. El magmatismo gondwánico. In: Ramos, V.A. (Ed.), Geología y Recursos Naturales de Mendoza. XII Congreso Geológico Argentino and II Congreso de Exploración de Hidrocarburos, Relatorio, I (6), 53–64.

Llambías, E.J., Quenardelle, S., Montenegro, T., 2003. The Choiyoi Group from central Argentina: a subalkaline transitional to alkaline association in the craton adjacent to the active margin of the Gondwana continent. Journal of South American Earth Sciences 16, 243–257.

López, V., Gregori, D.A., 2004. Provenance and evolution of the Guarguaraz Complex, Cordillera Frontal, Argentina. Gondwana Research 7 (4), 1197–1208.

Lopez, V.L., Escayola, M., Azarevich, M.B., Pimentel, M.M., Tassinari, C., 2009. The Guarguaraz Complex and the Neoproterozoic Cambrian evolution of southwestern Gondwana: geochemical signatures and geochronological constraints. Journal of South American Earth Sciences 28, 333–344.

Maksaev, V., Munizaga, F., Tassinari, C., 2014. Timing of the magmatism of the paleo-Pacific border of Gondwana: U-Pb geochronology of Late Paleozoic to Early Mesozoic igneous rocks of the north Chilean Andes between 20° and 31°S. Andean Geology 41 (3), 447–506.

Mirré, J.C., 1966. Geología del Valle del río de los Patos (entre Barreal y las Hornillas). Revista de la Asociación Geológica Argentina 21 (4), 211–232 (Buenos Aires).

Mora-Klepeis, G., McDowell, W.F., 2004. Late Miocene calc-alkalic volcanism in the northwestern Mexico: an expression of rift or subduction-related magmatism? Journal of South American Earth Sciences 17, 297–310.

Mpodozis, C., Kay, S., 1992. Late Paleozoic to Triassic evolution of the Gondwana margin: evidence from Chilean Frontal Cordillera batholiths (28°S to 31°S). Geological Society of America Bulletin 104, 999–1014.

Müller, D., Groves, D.I., 1995. Potassic Igneous Rocks and Associated Gold-Copper Mineralization. Lecture notes in Earth Sciences. Springer, 210 pp.

Orme, H., Petford, N., Atherton, M., Gregori, D., Ruviños, M., Pugliese, S., 1996. Petrology and Emplacement of Frontal Cordilllera Granitoids, Mendoza Province, Western Argentina (33–34° S), 3rd International Simposyum on Andean Geodynamics. St Malo, France, 613–616.

Pagani, M.A., Sabattini, N., 2002. Biozonas de moluscos del Paleozoico superior de la Cuenca Tepuel - Genoa (Chubut, Argentina). Ameghiniana 39 (3), 351–366.

Parada Velazquez, F.N., 2013. Geoquímica de las rocas ígneas del Carbonífero-Trásico de la Alta Cordillera, Region de Atacama, Chile. Memoria para optar a Título de Geólogo, Santiago de Chile, 94 pp.

Pearce, J.A., Harris, N.B.W., Tindle, A.G., 1984. Trace element discrimination diagrams for the tectonic interpretation of granitic rocks. Journal of Petrology 25, 956–983.

Pecerrillo, A., Taylor, S.R., 1976. Geochemistry of Eocene calcoalkaline volcanic rocks from the Kastamonu Area, Northern Turkey. Contributions to Mineralogy and Petrology 58, 63–81.

Polanski, J., 1958. El bloque Varíscico de la Cordillera Frontal de Mendoza. Revista de la Asociación Geológica Argentina 12, 165–193 (Buenos Aires).

Polanski, J., 1964. Descripción Geológica de la Hoja 25a, Volcán San José, Provincia de Mendoza. Boletín 98. Carta geológica-económica de la República Argentina. Ministerio de Ind y Minería. Dirección Nacional de Geología y Minería, Secretaria de Estado de Minería, Buenos Aires, 94 pp.

Poma, S., Ramos, V.A., 1994. Las secuencias básicas iniciales del Grupo Choiyoi, Cordón del Portillo, Mendoza: Sus implicancias tectónicas. VII Congreso Geológico Chileno Actas II, 1162–1166 (Concepción. Chile).

Pöthe de Baldis, E.D., 1975. Triásico. Serie Porfirítica y Carbónico en la Comarca de Cerro Cantera, Uspallata, Mendoza. II Congreso Ibero-Americano de Geología Económica Actas 4, 7–24 (Buenos Aires).

Ramos, V.A., 1988. The tectonics of the Central Andes: 30° to 33° S latitude. In: Clark, S., Burchfield, D. (Eds.), Processes in Continental Lithospheric Deformation, Special Paper Geological Society of America, vol. 218, pp. 31–54 (Boulder).

Rolleri, E.O., Criado Roque, P., 1970. Geología de la provincia de Mendoza. IV Jornadas Geológicas Argentinas (Mendoza, 1969) Actas II, 1–60 (Buenos Aires).

Rubinstein, C.V., Steemans, P., 2007. New palynological data from the Devonian Villavicencio Formation, Precordillera of Mendoza, Argentina. Ameghiniana 44, 3–9.

Sabattini, N., 1993. Invertebrados Neopaleozoicos. Relatorio XII Congreso Geologico Argentino and II Congreso de Exploración de Hidrocarburos. Geología y recursos naturales de Mendoza. Ramos V.A. (Ed.), Relatorio, 2(7): 297–302.

Sato, A.M., Llambías, E.J., 1993. El Grupo Choiyoi, provincia de San Juan: equivalente del Batolito de Colangüil. XII Congreso Geológico Argentino Actas 4, 156–165 (Mendoza).

Stipanicic, P.N., Rodrigo, F., Baulíes, O.L., Martínez, C.G., 1968. Las formaciones presenonianas en el denominado Macizo Nordpatagónico. Asociación Geológica Argentina, Revista XXIII (2), 67–98 (Buenos Aires).

Strazzere, L., Gregori, D., 2005. Interpretación de la sucesión volcaniclástica del Grupo Choiyoi en la Quebrada de Santa Elena, Precordillera de Mendoza, Argentina. Revista de la Asociación Geológica Argentina 60 (3), 486–494.

Strazzere, L., Gregori, D., Dristas, J., 2006. Genetic evolution of Permo-Triassic volcaniclastic sequences at Uspallata, Mendoza Precordillera, Argentina. Gondwana Research 9, 485–499.

Sun, S.S., McDonough, W.F., 1989. Chemical and isotopic systematics of oceanic basalts: implications for mantle composition and processes. In: Saunders, A.D., Norry, M.J. (Eds.), Magmatism in the Ocean Basins, Geological Society of London, Special Publication, vol. 42, pp. 313–345.

Taboada, A.C., 2001. Bioestratigrafía del Neopaleozoico del Valle de Tres Lagunas, Sierra de Tepuel, provincia de Chubut. Acta Geológica Lilloana, Tucumán 18 (2), 291–304.

Thompson, R.N., 1982. British Tertiary volcanic province. Scottish Journal of Geology 18, 49–107.

Thompson, R., Mitchell, J.C., 1972. Palaeomagnetic and radiometric evidence for the age of the lower boundary of the Kiaman magnetic interval in South America. Geophysics Journal Royal Astronomic Society 27, 207–214.

Varela, R., 1973. Estudio geotectónico del extremo sudoeste de la Precordillera de Mendoza, República Argentina. Revista de la Asociación Geológica Argentina 28 (3), 241–267 (Buenos Aires).

Willner, A.P., Gerdes, A., Massonne, H.J., Schmidt, A., Sudo, M., Thomson, S., Vujovich, G., 2011. The geodynamics of collision of a microplate (Chilenia) in Denovian times deduced by the pressure-temperature-time evolution within part of a collisional belt (Guarguaraz Complex, W-Argentina. Contributions to Mineralogy and Petrology 162, 303–327.

Winchester, J.A., Floyd, P.A., 1977. Geochemical discrimination of different magma series and their differentiation products using immobile elements. Chemical Geology 20, 325–343.